https://doi.org/10.5194/egusphere-2023-2655
Preprint. Discussion started: 5 February 2024

New age constraints reveal moraine stabilization thousands of years after deposition during the last deglaciation of western New York, USA

Karlee K. Prince[1], Jason P. Briner[1], Caleb K. Walcott[1], Brooke M. Chase[1], Andrew L. Kozlowski[2], Tammy M. Rittenour[3], Erica P. Yang[1,4]

[1] Department of Geology, University at Buffalo, 126 Cooke Hall, Buffalo, NY 14260, USA
[2]New York State Geological Survey, New York State Museum, 222 Madison Ave, Albany, NY 12230, USA
[3]Department of Geoscience, Utah State University, 4505 Old Main Hill, Logan, UT 84322, USA
[4]Oak Ridge Institute of Science and Education, 1299 Bethel Valley Road, Oak Ridge, TN, 37830 USA

Correspondence to: Karlee K. Prince (karleepr@buffalo.edu)

https://doi.org/10.5194/egusphere-2023-2655
Preprint. Discussion started: 5 February 2024

Abstract. The timing of the last deglaciation of the Laurentide Ice Sheet in western New York is poorly constrained. The lack of direct chronology in the region has led to a provocative hypothesis that the Laurentide Ice Sheet re-advanced to near its Last Glacial Maximum terminal position in western New York at ~13 ka, which challenges long-standing datasets. To address this hypothesis, we obtained new chronology from the Kent (terminal) and Lake Escarpment (first major recessional) moraines using radiocarbon ages in basal sediments from moraine kettles supplemented with two optically stimulated luminescence ages. The two optically stimulated luminescence ages date the Kent (terminal) position to 19.8 ± 2.6 and 20.6 ± 2.9 ka. Within the sediment cores from both moraines, the lowest reliable radiocarbon ages range from 15,000-15,400 to 13,600-14,000 cal yr BP. Below these dated levels is sedimentologic evidence of an unstable landscape during basin formation; radiocarbon ages from these lowest sediments are not in stratigraphic order and date from 19,350-19,600 to 14,050-14,850 cal yr BP. The oldest radiocarbon age of 19,350-19,600 cal yr BP – from a rip-up clast – suggests ice-free conditions at that time. We interpret that the 5 kyr lag between the optically stimulated luminescence ages and the lowest reliable radiocarbon ages is the result of persistent buried ice in ice-cored moraines until ~15 to 14 ka. The cold conditions associated with Heinrich Stadial 1 may have enabled the survival of ice-cored moraines in permafrost until after 15 ka, and in turn, climate amelioration during the Bølling Period (14.7 – 14.1 ka) may have initiated landscape stabilization. This model potentially reconciles the sedimentological and chronological evidence underpinning the provocative re-advance hypothesis, which instead could be the result of moraine instability during the Bølling-Allerød periods (14.7 – 13 ka). Age control for future work should focus on features that are not dependent on local climate.

1 Introduction

Much glacial research over the last century has focused on the style and timing of Laurentide Ice Sheet (LIS) recession from the Great Lakes region of North America following the Last Glacial Maximum (LGM, 26-19 ka; Dalton et al., 2020; Dyke, 2004; Fairchild, 1909). Well constrained ice sheet chronologies are necessary to constrain the timing of meltwater re-routing events from ice-dammed lakes that occupied the Great Lakes basins during the last deglaciation (Barth et al., 2019; Calkin and Feenstra, 1985; Leydet et al., 2018; Porreca et al., 2018; Rayburn et al., 2007), as these events are hypothesized to have had significant climatic impacts (Broecker et al., 1989; Donnelly et al., 2005). Models that attempt to understand past climate change (Osman et al., 2021), ice sheet sensitivity (Briner et al., 2020), and atmospheric organization (Löfverström et al., 2014; Tulenko et al., 2020) all require paleo ice sheet configurations. Therefore, well-defined ice sheet retreat chronologies are critical for understanding dynamics and forcings within the late glacial climate system.

Despite the critical need for precise chronologies of ice margin retreat of the LIS in the Great Lakes region, ice margin reconstructions in western New York lack detailed age control. Here, there are no local ages on the terminal moraine and few from the recessional moraines (Muller and Calkin, 1993), leaving the deglacial chronology to be largely based on correlations with dated moraines and proglacial shorelines to the west in Ohio and to the east in New York (Fullerton, 1980; Ridge, 2003). These correlations suggest that the western New York Kent (terminal) and Lake Escarpment (recessional) moraines date to ~20 and 17 ka, respectively (Fig. 1). However,

https://doi.org/10.5194/egusphere-2023-2655
Preprint. Discussion started: 5 February 2024

Young et al. (2020) recently interpreted new radiocarbon ages from western New York to support a significant re-advance of the LIS at ~13 ka that overtopped the Lake Escarpment Moraine and nearly reached the Kent Moraine (Fig. 1). In contrast to Young et al.'s (2020) reconstruction, most literature places the LIS margin north of Lake Ontario at this time (Dalton et al., 2020; Muller and Calkin, 1993; Terasmae, 1980; and references therein), with the drainage of Glacial Lake Iroquois occurring at ~13 ka (Fig. 1; Cronin et al., 2012; Lewis and Anderson, 2019; Rayburn et al., 2005). If a re-advance of the scale hypothesized by Young et al. (2020) occurred (henceforth referred to as the 'Allerød re-advance hypothesis'), we would need to revisit many regional deglaciation chronologies.

To further constrain moraine ages in western New York and to test the Allerød re-advance hypothesis, we obtained 23 new macrofossil-based radiocarbon ages from five sediment cores collected on the Kent Moraine, and 18 new macrofossil-based radiocarbon ages from two sediment cores on the Lake Escarpment Moraine. The Lake Escarpment Moraine is within the extent of the proposed re-advance, so if basal ages from sites on this moraine pre-date ~13 ka, and the subsequent stratigraphy shows no evidence of a re-advance, then the evidence would refute the Allerød re-advance hypothesis. Conversely, basal radiocarbon ages that post-date ~13 ka, and/or evidence that the sediment stratigraphy is interrupted at ~13 ka, would support an Allerød re-advance. Additionally, we obtained two optically stimulated luminescence (OSL) ages from kame delta sediments associated with deposition of the Kent Moraine to provide a more complete understanding of deglaciation. Our results provide new chronological constraints in the western New York data gap, and do not support the ~13 ka re-advance proposed by Young et al. (2020). Rather, our data support a model of initial moraine deposition followed by thousands of years before kettle basin formation and final moraine stabilization.

https://doi.org/10.5194/egusphere-2023-2655
Preprint. Discussion started: 5 February 2024

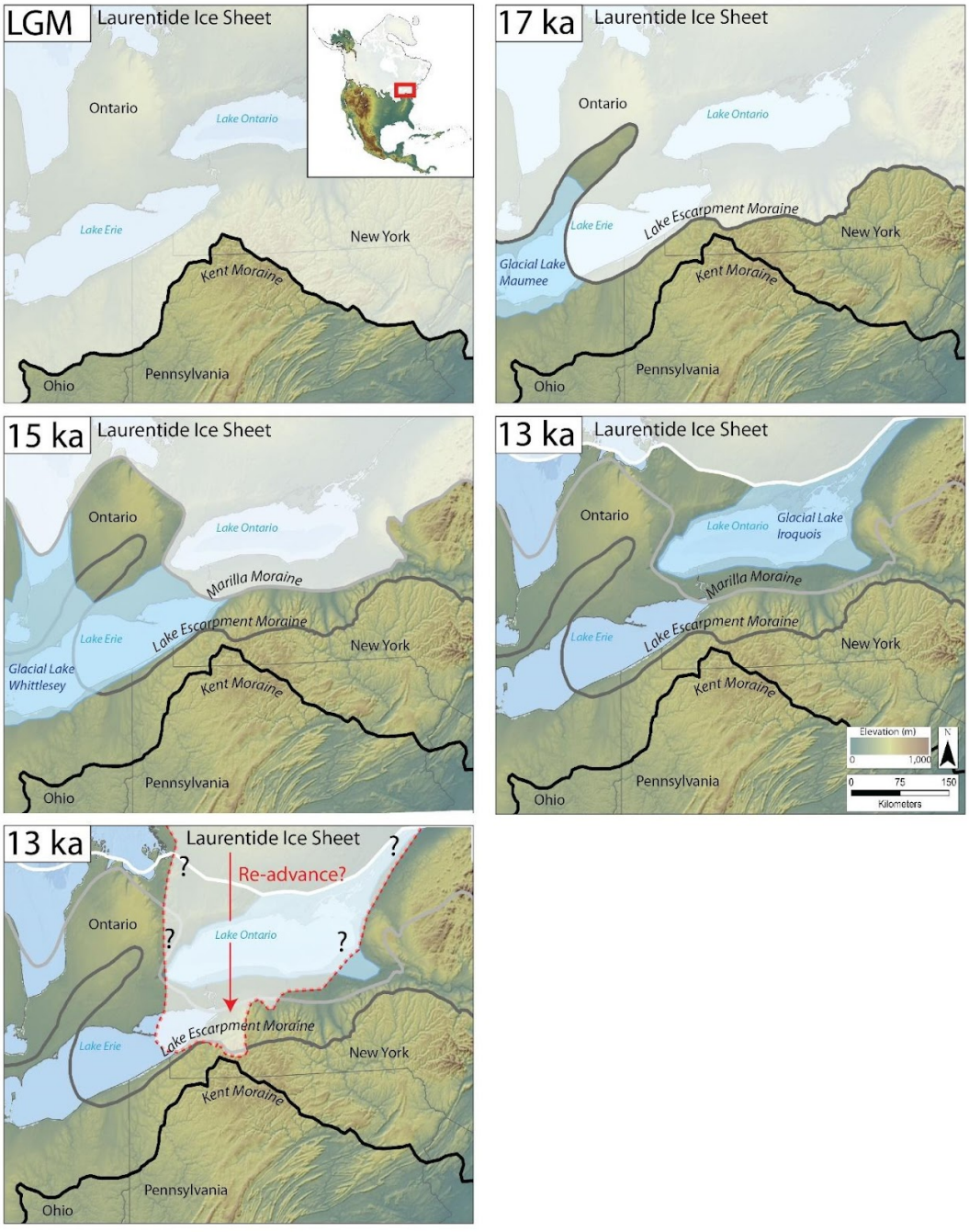

Figure 1. Map depictions of the deglaciation of the eastern Great Lakes after the Last Glacial Maximum. Black line is the Kent Moraine, modified from Dalton et al. (2020), the 'Pennsylvania Department of Conservation and Natural Resources Late Wisconsin Glacial Border' (https://www.pasda.psu.edu), and the 'Quaternary Geology 500K - Glacial Boundary of Ohio' (https://gis.ohiodnr.gov). Dark gray line is the 17 ka ice margin from Dalton et al. (2020) which depicts the Lake

https://doi.org/10.5194/egusphere-2023-2655
Preprint. Discussion started: 5 February 2024

Escarpment Moraine. Light gray line is the 15 ka ice margin from Dalton et al. (2020) which depicts the Marilla Moraine. Glacial Lake Maumee and Whittlesey are included for general reference, and derived with shoreline elevations (Fisher et al., 2015). White line is the 13 ka ice margin from Dalton et al. (2020) and we estimated Glacial Lake Iroquois using Bird and Kozlowski (2016). Red dashed line depicts a hypothesized ice sheet configuration to explain the hypothesis presented in Young et al. (2020). Note that the LIS would dam a pro-glacial lake in the Lake Erie basin and overrun several moraine belts, including the Lake Escarpment Moraine. DEM from U.S. Geological Survey's Center for Earth Resources Observations and Science (EROS).

2 Geologic Setting

The Kent Moraine in western New York is correlated to the Kent Moraine in northwest Ohio, the Olean Moraine in Pennsylvania, the Harbor Hill Moraine in New Jersey, and the Martha's Vineyard Moraine in Massachusetts (Fig. 1; Balco et al., 2002; Fullerton, 1980; Muller and Calkin, 1993; Stanford et al., 2020). Retreat from the LGM moraine in these adjacent regions is dated to 19.8 ± 0.4 ka in Ohio (Glover et al., 2011), 25.2 ± 2.1 ka (Corbett et al., 2017) and 23,200-23,750 cal yr BP in New Jersey (Stanford et al., 2020), and 25.5 ± 0.4 ka in Massachusetts (Balco et al., 2009; Balco et al., 2002). Therefore, we infer that the Kent Moraine in western New York was likely deposited sometime between 25 and 20 ka.

The first major moraine belts deposited after the maximum LGM position were the Ashtabula Moraine in Ohio and northwest Pennsylvania, the Lake Escarpment Moraine in western New York, and Valley Heads moraines in central New York (Fig. 1; Fullerton, 1980; Muller and Calkin, 1993). During this ice position, Glacial Lake Maumee occupied the Lake Erie basin, and is dated to 17 - 16 cal ka BP by radiocarbon dating at the paleo-outlet and OSL dating of strandlines (Calkin and Feenstra, 1985; Eschman and Karrow, 1985; Fisher et al., 2015). Ridge (2003) tied the outer and inner Valley Heads moraines to the New England Varve Chronology, placing these moraines at 17,200 and 16,200 cal yr BP, respectively. Kozlowski et al. (2018) report basal ages of 14,300-14,900 and 14,200-14,850 cal yr BP from basins within the outer Valley Heads limit. These ages are younger than previous estimates, leading Kozlowski et al. (2018) to suggest the moraine may have been re-occupied. Calkin and McAndrews (1980) report minimum-limiting radiocarbon ages of 13,750-15,250 cal yr BP from wood stratigraphically above outwash sands from Nichols Brook in western New York (Fig. 2). Muller and Calkin (1993) extrapolated their ages to estimate ~17,600 cal yr BP for the emplacement of the outwash.

Following the deposition of the Lake Escarpment Moraine, Glacial Lakes Whittlesey and Warren occupied the Lake Erie basin between 16 and 14 ka (Fig. 1; Fullerton, 1980; Muller and Calkin, 1993). The lowering of Glacial Lake Whittlesey to Glacial Lake Warren is dated to 14,150-15,550 cal yr BP at Winter Gulf in western New York (Fig. 2; Calkin and McAndrews, 1980), and Warren strandlines in northwest Ohio have been dated to 14.2 ± 1.3 ka (Higley et al., 2014) and 14.1 ± 1.0 ka in (Campbell et al., 2011). These proglacial lake chronologies provide unambiguous minimum age constraints of >15 ka for the deposition of the Lake Escarpment Moraine.

The LIS continued its northward retreat and formed Glacial Lake Iroquois from 14.7 to 13.0 ka in the Lake Ontario basin (Fig. 1; Muller and Calkin, 1993; Muller and Prest, 1985; Teller, 2003). The switch of the Glacial Lake Iroquois spillway from the Mohawk River valley to the lower outlet at Covey Hill is constrained between 13,200 and 13,000 cal yr BP by numerous radiocarbon constraints from the pre- and post-flood histories of Lake

https://doi.org/10.5194/egusphere-2023-2655
Preprint. Discussion started: 5 February 2024

Vermont and Lake Iroquois (Lewis and Anderson, 2019; Rayburn et al., 2007; Richard and Occhietti, 2005). Similarly, the formation of the Champlain Sea occurred between 13,100 and 12,700 cal yr BP, which post-dates the final draining of Glacial Lake Iroquois and requires an ice margin north of the Lake Ontario outlet (Cronin et al., 2012; Rayburn et al., 2011). Collectively, this ice recession chronology is at odds with the Allerød re-advance hypothesis, with its significant LIS advance across the Lake Ontario basin and to near the terminal moraine in western New York ~13 ka (Fig. 1; Young et al., 2020).

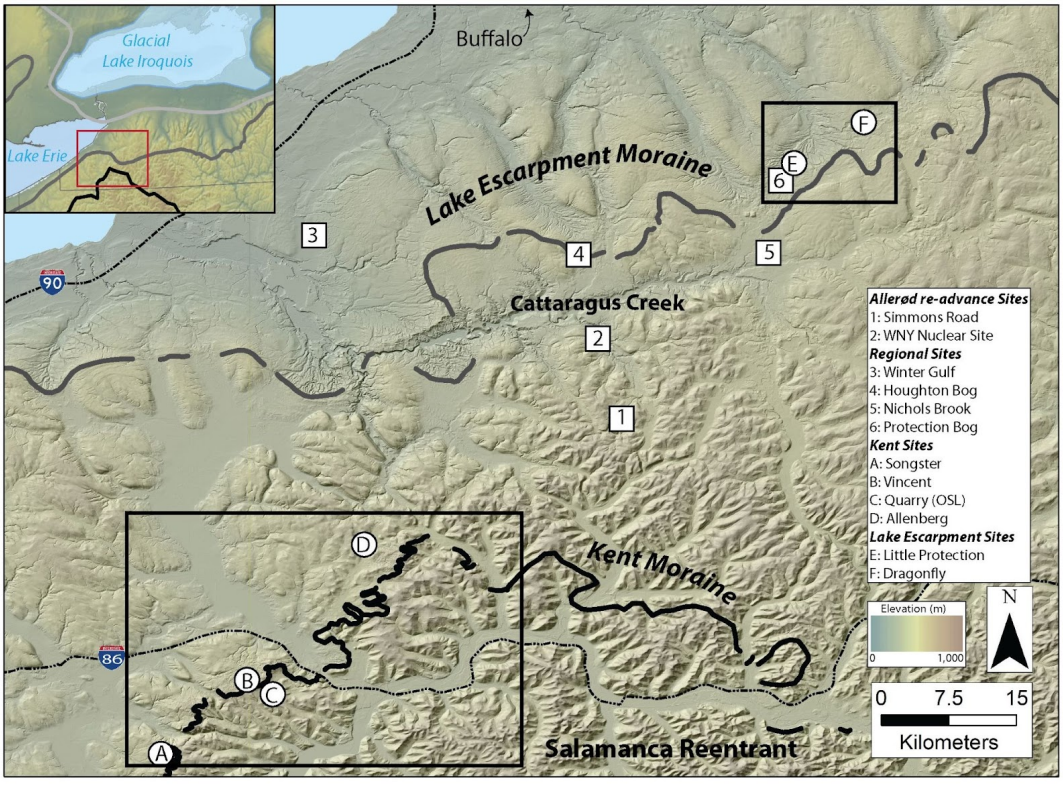

Figure 2. Study sites in relation to previously published work. Black and gray lines are the same as in Fig. 1. Squares 1 and 2 depict hypothesized sites overrun by the Allerød re-advance at 13 ka (Young et al., 2020). Circles A-D are our sites on the Kent Moraine. Circles E and F are our sites on the Lake Escarpment Moraine. Squares 3-6 are Winter Gulf and Nichols Brook (Calkin and McAndrews, 1980), and Houghton and Protection Bog (Miller, 1973). The two black boxes show the extent of the maps in Fig. 3. DEM from U.S. Geological Survey's Center for Earth Resources Observations and Science (EROS).

3 Methods

3. 1 Sediment cores

Our primary approach for constraining the timing of deglaciation and testing the Allerød re-advance hypothesis was obtaining basal sediment ages from kettles within the Kent and Lake Escarpment Moraines. Newly

https://doi.org/10.5194/egusphere-2023-2655
Preprint. Discussion started: 5 February 2024

available light detection and ranging (LiDAR)-based bare-Earth 1-m digital elevation models (DEMs) enabled us to identify natural kettle basins (Fig. 3). Typically, moraines in western New York have both single ridges where the ice sheet abutted higher topography, and hummocky morainal belts that contain numerous kettle basins. Kame deltas exist in places where the ice sheet dammed adjacent river valleys. The hummocky nature of most moraines indicates that the moraines were ice-rich when deposited (Fig. 3).

We collected sediment cores from kettles that presently range from bogs to wetlands. We cored five sites on the Kent Moraine referred to as the Vincent-1 (core name: 20VIN1), Vincent-3 (20VIN3), Vincent-4 (20VIN4), Songster (21SONG1), and Allenberg (15ABB7) sites (Table 1, Fig. 3), and two sites on the Lake Escarpment Moraine referred to as the Little Protection (21LPB1) and Dragonfly (13DFK1) sites (Table 1, Fig. 3). All sites are within hummocky moraine.

We determined basin depocenters using thin steel rods to measure the depth of the organic sediment infill. We used Livingstone- and Russian Peat-style corers to collect organic-rich sediment infill, and a manual percussion GeoProbe system to collect the underlying stiff, minerogenic sediments. From some sites, our sediment cores extended from the present surface to mineral-rich sediments below the organic-sediment infill; from others, our sediment cores began and ended at depth, spanning the organic-to-mineral sediment contact and downward until we penetrated coarse deposits (Table 1). We returned and cored the Vincent-1 and -4 sites multiple times to collect the entire sequence.

We split, imaged, and generated downcore data on all sediment cores at the University at Buffalo. We measured magnetic susceptibility in contiguous 1 cm intervals using a Bartington MS2E High Resolution Surface Scanning Sensor scanner connected to a Bartington MS2 Magnetic Susceptibility Meter to assess the minerogenic content. We calculated loss-on-ignition (LOI) percent by burning ~1 cm^3 of sediment in a Thermolyne Muffle Furnace at successively higher temperatures for water (105°C), organic carbon (550°C), and carbonate (950°C) content to help characterize the sediment units and depositional setting (Heiri et al., 2001; Last and Smol, 2001). To calculate composite core length, we spliced together overlapping sediment sections using visual lithologic changes and magnetic susceptibility measurements. We volumetrically sampled portions of the Little Protection sediment cores to determine sediment bulk density.

We use radiocarbon dating of macrofossils for age control (Table 2). The sediments are organic-rich in the upper portions of the cores and are organic-poor in the lower sections. Where available, we picked full plant macrofossils. We picked macrofossils that were from the center of the sediment core and demonstrably in-situ. In macrofossil-devoid sections, we wet sieved sediment with deionized water to isolate and combine the largest macrofossil fragments for dating. We attempted to identify macrofossils, but some macrofossil fragments were small and unidentifiable (Table 2). We rinsed samples with deionized water, freeze-dried them, and sent samples to the National Ocean Sciences Accelerator Mass Spectrometry (NOSAMS) or the Keck Lab at the University of California Irvine (KCCAMS) for radiocarbon analysis. We submitted untreated macrofossils, therefore the facilities conducted acid-base-acid (ABA) pretreatments, converted samples to graphite, and ran them on the AMS (Elder et al., 2019; Olsson, 1986; Pearson et al., 1997; Shah Walter et al., 2015; Vogel et al., 1984).

https://doi.org/10.5194/egusphere-2023-2655
Preprint. Discussion started: 5 February 2024

We report the entire 2σ age range and round ages according to Stuiver and Polach (1977) (Table 2) We calibrated all the radiocarbon results using Calib8.1 with the IntCal20 dataset (Reimer et al., 2020; Stuiver and Reimer, 1993). $\delta^{13}C$ measurements were measured on a split of the CO_2 gas generated from each sample on an isotope-ratio mass spectrometer. Uncertainties in the $\delta^{13}C$ from both labs are <0.1‰. We report $\delta^{13}C$ values as ‰ VPDB.

Table 1: Site location, core lengths, and ownership.

Site Name	Core Name	Latitude (DD)	Longitude (DD)	Elevation (m asl)	Site Length (m)	Core Top (m bg)	Core Bottom (m bg)	Property Ownership
Vincent 1	20VIN1	42.109	-79.000	596	145.0	0.0	6.6	Vincent Family
Vincent 3	20VIN3	42.110	-78.999	593	39.0	1.5	2.9	Vincent Family
Vincent 4	20VIN4	42.109	-78.999	594	81.0	3.1	5.4	Vincent Family
Songster	21SONG1	42.040	-79.079	581	172.0	4.1	4.8	Songster Family
Allenberg	15ABB7	42.252	-78.883	524	321.0	8.0	14.6	Buffalo Audubon Society
Little Protection	21LPB1	42.621	-78.463	440	228.0	0.0	8.1	Erie County Parks Dept.
Dragonfly	13DFK1	42.679	-78.386	450	117.0	0.0	7.3	Buffalo Audubon Society
Corbett Hill	-	42.114	-78.946	530	-	-	-	JMI Corbett Hill Gravel

DD: Decimal Degrees
asl: Above sea level
bg: Below ground

https://doi.org/10.5194/egusphere-2023-2655
Preprint. Discussion started: 5 February 2024

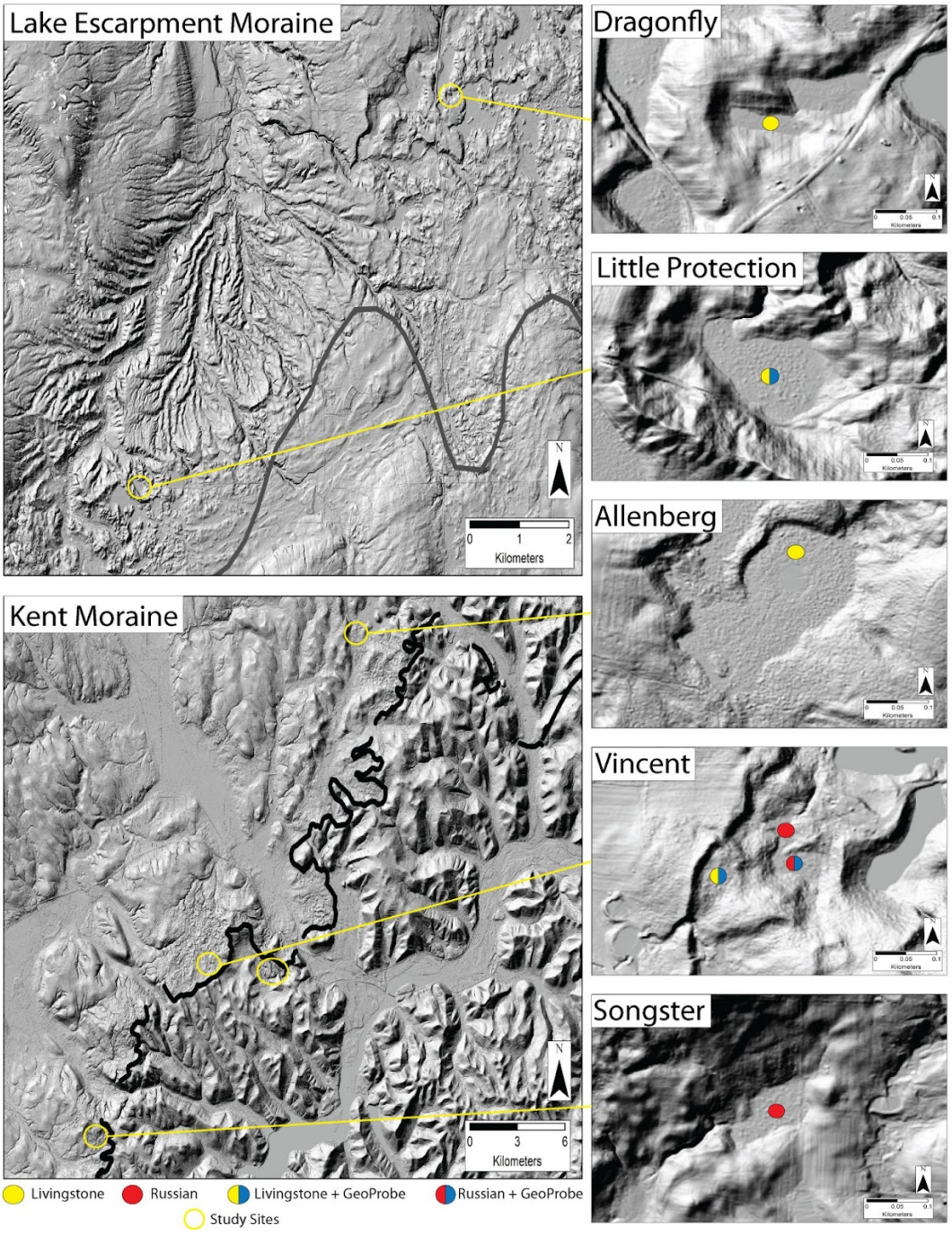

Figure 3. Site maps of the sediment core locations. 1-m bare-Earth DEM hillshade from https://data.gis.ny.gov/ with the Kent (black) and Lake Escarpment (gray) moraines. Open yellow circles depict study site location and yellow lines

https://doi.org/10.5194/egusphere-2023-2655
Preprint. Discussion started: 5 February 2024

associate each site location with a site map. Figure 4 contains the site map for the open yellow circle with no associated site map. The filled circles indicate the type of coring device used in each site and the coring location. The filled yellow circles depict where we used a Livingstone. The filled red circles depict where we used a Russian Peat Corer. The filled semi-circles indicate where we used a Livingston or Russian Peat Corer in the soft sediment infill and then used the GeoProbe in the stiff minerogenic sediment.

3.2 Optically stimulated luminescence dating

We collected sediment samples for OSL dating from topset beds within an ice-contact delta deposit associated with the Kent Moraine to determine when the LIS was present at this location (Fig. 3 & 4). Our sample location was Corbett Hill Gravel Quarry, an active aggregate quarry that exposes large sedimentary sequences indicative of a proglacial delta. The sediments consisted of cobble-rich foreset beds overlain by ~3 m of near-horizontal topset beds. We collected sand samples for OSL dating from the topset sequence ~2.1 m below the delta surface. We created a fresh exposure of the topset beds with an excavator, exposing alternating layers of gravels and coarse sands, with lenses of medium/fine-sand and silt. We collected two samples for OSL dating in fine-sand lenses in 5.1 x 25.4 cm (2 x 10 inch) aluminum tubes after clearing back outer sediments (Fig. 4). Samples for water content and dose rate determination were collected from surrounding sediments.

We processed the samples at the Utah State University Luminescence Laboratory for small aliquot OSL dating of fine-grained quartz sand (Table 3, ATable 1). First, we purified samples to 150-250 μm quartz sand using wet sieving, and chemical treatment with 10% hydrochloric acid to remove carbonates, 5% peroxide to remove organics, 2.72 g/cm^3 sodium polytungstate to remove heavy minerals and 48% hydrofluoric acid to remove feldspars and etch the quartz grains. We analyzed small aliquots of quartz (0.4 to 1 mm diameter of sand mounted on disk, ~10-20 grains) on Risø DA-20 readers, using the single-aliquot regenerative-dose (SAR) protocol (Murray and Wintle, 2000). We analyzed 42 aliquots for sample 21SICK-01 and 37 for sample 21SICK-02, of which we used 21 and 23 aliquots for age calculations, respectively (Fig. A1 & A2). Aliquots were rejected from age calculation if they showed signal depletion with infrared stimulation indicating feldspar contamination (0-12 aliquots), poor recycling of a repeat point (greater than 80% difference between repeat points, 7-8 aliquots), high recuperation of a zero-dose point (>10% of the Natural signal, 0-6 aliquots), extrapolation of the equivalent dose beyond the dose-response curve (0-2 aliquots) and poor dose-response curve fit (0-3 of aliquots). We applied a minimum age model (MAM) to the samples to calculate our equivalent does (D_E; Grays; Gy, Fig. A1 & A2), as used by similar studies on LIS glaciofluvial terraces elsewhere in the northern United States (Rittenour et al., 2015).

We determined the dose rate for OSL age calculation based on U, Th, K, and Rb concentrations from the surrounding sediments using inductively coupled plasma-mass spectrometry and atomic emission spectrometry. Using the conversion factors of Guérin et al. (2011), we converted elemental concentrations to dose rate. The contribution of cosmic radiation was based on sample depth, elevation and latitude following Prescott and Hutton (1994). We also determined water content by measuring the mass of the samples before and after desiccation. With these three factors, we were able to calculate environmental dose rates (Gy/kyr). Our reported OSL ages are simply the D_E (determined with the MAM) divided by the dose rate with 1σ standard error (Table 3). We report ages with 1σ uncertainty (Table 3).

https://doi.org/10.5194/egusphere-2023-2655
Preprint. Discussion started: 5 February 2024

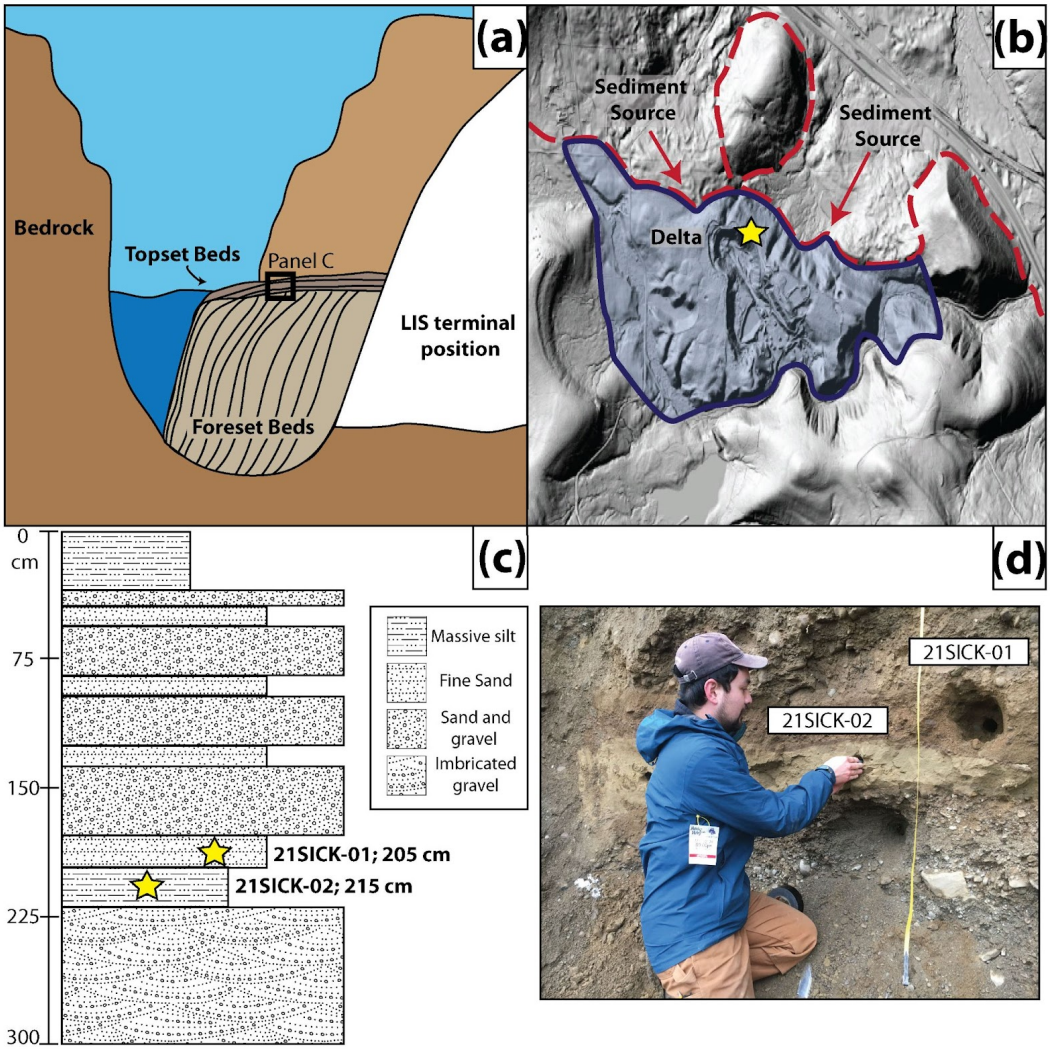

214

215 **Figure 4. Panel A) is a schematic of the kame delta creation. The LIS dammed a lake and deposited the delta outboard of**
216 **the Kent Moraine. B) is a 1-m DEM hillshade showing the kame delta outboard of the Kent Moraine (within the open**
217 **yellow circle in Fig. 3). Red dashed line depicts the extent of the Kent Moraine. Red arrows depict the sediment source for**
218 **the delta. Blue line and shading depicts the delta deposit. Yellow star on the side of the active quarry shows our sampling**
219 **site. C) shows a stratigraphic column of the topset beds. We use the FGDC Digital Cartographic Standard for Geologic**
220 **Map Symbolization (U.S. Geological Survey). Yellow stars show our sampling location. D) is a field photo of the**
221 **stratigraphic section showing the location of our two samples.**

222

https://doi.org/10.5194/egusphere-2023-2655
Preprint. Discussion started: 5 February 2024

4 Results

4.1 Stratigraphy

The sediment cores contain three stratigraphic units: a basal unit (Unit 1) of diamicton, an intermediate unit (Unit 2) dominated by silt and sand, and an upper unit (Unit 3) of organic-rich silt and peat (Fig. 5). We only recovered Unit 1 in 20VIN1 using the Geoprobe system (Fig. 5). Unit 1 is a gray massive pebbly diamicton with a silty matrix. The contact with Unit 2 is sharp.

We collected varying thicknesses of Unit 2 (Fig. 5). Unit 2 is mineral-rich layers with complex stratigraphy and sparse macrofossil fragments. In 20VIN1, Unit 2 is layered gray sand and silt that grades to alternating massive brown and gray silt (Fig. 5). In 20VIN3, Unit 2 begins as gray silt, transitions to a light brown silt, and is topped by gray clay. In 20VIN4, Unit 2 contains alternating layers of pebbly diamicton (with some clasts up to 5 cm long) and silty clay. The contacts between the layers are sharp and one is undulating. In 21LPB1, Unit 2 begins with 2 cm of gray silty gravel before a sharp contact with massive, oxidized sand and gravel. Above this is a sharp transition to alternating layers of gray silt, silty gravel, and sand; these layers have sharp and sometimes undulating contacts. That is overlain by massive gray clay. In 13DFK1, Unit 2 is gray silt. The contact between Unit 2 and 3 is sharp in all cores.

Unit 3 is organic-rich silt (lower Unit 3) and peat (upper Unit 3) that spans from the mineral layers of Unit 2 to the top of each sediment sequence. The transition from organic-rich silt to peat is sharp in all cores. In 20VIN1, within the initial sediments of Unit 3, there are three layers of gray silt and an inclusion of gray clay that are identical to the sediment of Unit 2. Similarly, 20VIN3 has a layer of gray silt within the initial organic-rich silt. The organic-rich silt and peat have high organic carbon content and large macrofossils are common.

To address the Allerød re-advance hypothesis and seek evidence of whether the kettle sediments were overridden, we measured dry bulk density at 1-cm-resolution through the time interval of hypothesized re-advance in our Little Protection site core (21LPB1). The bulk density decreases from 1.55 g/cm^3 to 0.42 g/cm^3 in the transition from Unit 2 to 3. (Fig. 5) The density decreases due to the transition from minerogenic silt to organic-rich silt and remains below 0.42 g/cm^3 into Unit 3.

https://doi.org/10.5194/egusphere-2023-2655
Preprint. Discussion started: 5 February 2024

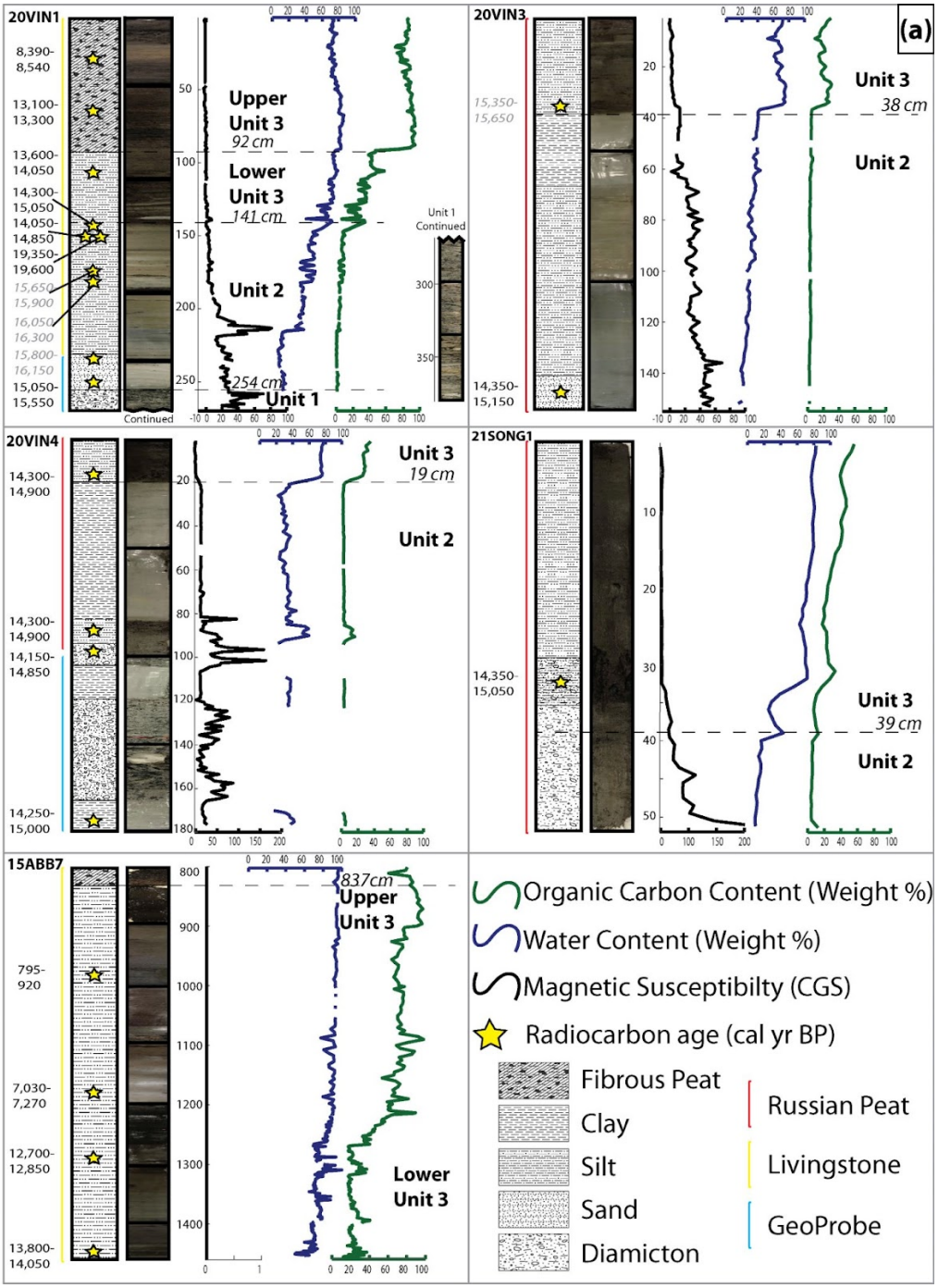

249

https://doi.org/10.5194/egusphere-2023-2655
Preprint. Discussion started: 5 February 2024

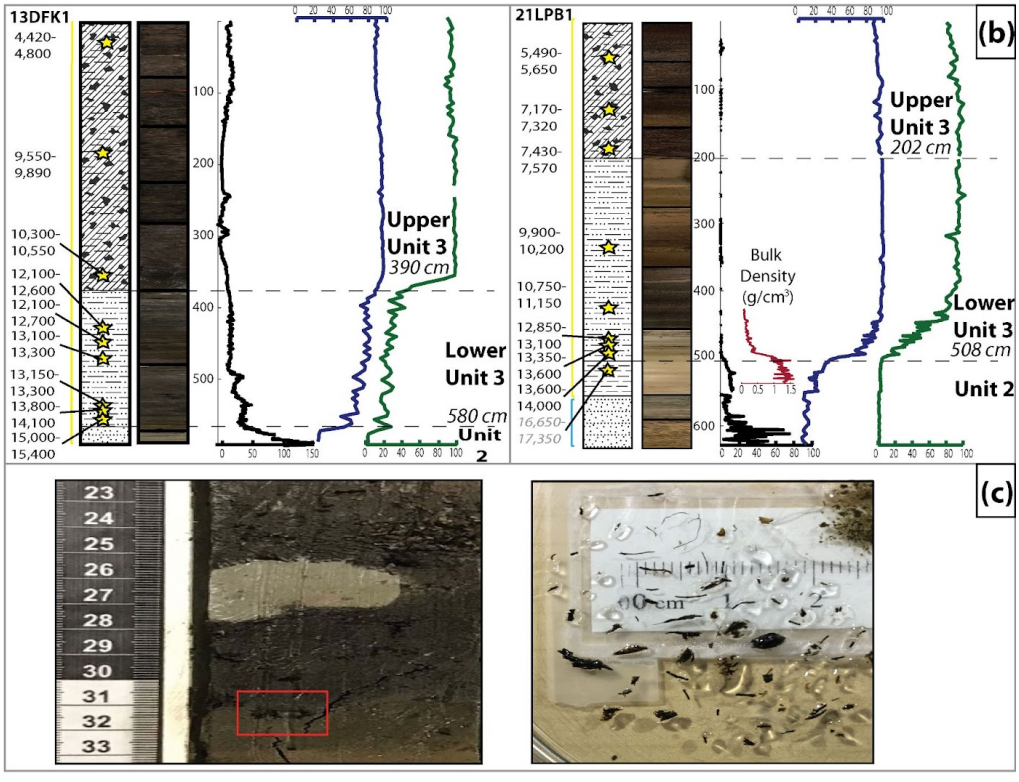

Figure 5. Panel A) has the sediment core stratigraphy from the Kent Moraine sites, and B) has the sediment core stratigraphy from the Lake Escarpment Moraine sites. We show sediment texture next to the core images using the FGDC Digital Cartographic Standard for Geologic Map Symbolization (U.S. Geological Survey). We plot magnetic susceptibility (CGS; black line), water content (weight %; blue line), and organic content (weight %, green line) by composite depth (cm). The colored line next to the stratigraphic column depicts if we used the Russian Peat Corer (red), Livingstone Corer (yellow), or GeoProbe (blue). Yellow stars indicate radiocarbon ages (2σ uncertainty cal yr BP). We used gray text and italics for radiocarbon ages we suspect have hardwater contamination. C) is a close-up image of the inferred gray clay and macrofossil-rich rip-up clasts in the transition from Unit 2 to 3 in 20VIN1 (shown in red box). The black box has post-sieve macrofossils from the rip-up clast in the red box.

4.2 Sediment core chronology

The stratigraphically lowest ages, or basal ages, from the Kent Moraine range from 15,050-15,550 to 13,800-14,050 cal yr BP (Table 2; Fig. 5). For 20VIN3, 20VIN4, and 21SONG1, the basal ages cluster around 14,700 cal yr BP. The basal ages from the Lake Escarpment Moraine are 15,000-15,400 and 16,650-17,350 cal yr BP. The basal ages are not the oldest ages, however. 20VIN1 has a basal age of 15,050-15,550 cal yr BP, yet is stratigraphically below other ages from Unit 2 of 15,650-15,900, 15,800-16,150, and 16,050-16,300 cal yr BP.

https://doi.org/10.5194/egusphere-2023-2655
Preprint. Discussion started: 5 February 2024

Furthermore, 110 cm higher than the basal age, there is an inclusion of macrofossils within Unit 2 that was dated twice and yields two radiocarbon ages of 19,350-19,600 and 14,050-14,850 cal yr BP; combined macrofossils from the surrounding sediment produce an age of 14,300-15,050 cal yr BP. In 20VIN3, the basal age is 14,350-15,150 cal yr BP, yet combined macrofossils higher in the core, at the Unit 2/3 boundary, produce an age of 15,350-15,650 cal yr BP.

https://doi.org/10.5194/egusphere-2023-2655
Preprint. Discussion started: 5 February 2024

Table 2: Radiocarbon dates for each study site. Listed by depth.

Lab Code	Depth (cm)	Fraction Modern	Fraction Modern Error	Mass (mg)	Material Dated	$\delta^{13}C$‰	^{14}C (yr)	^{14}C error (yr)	2 σ age range (cal BP)		Median (cal BP)
Vincent-1 (20VIN1)											
OS-164770	27.3	0.3854	0.0015	5.8	Wood	-26.50	7,660	30	8,390	8,540	8,440
OS-164771	67.3	0.2441	0.0015	5.8	Twig	-28.67	11,350	50	13,100	13,300	13,250
OS-164772	109.5-111.0	0.2263	0.0016	75.7	*Picea* seeds	-22.96	11,950	55	13,600	14,050	13,850
OS-164773	145.0	0.2105	0.0016	2.3	Unidentifiable	-24.32	12,500	60	14,300	15,050	14,700
UCIAMS-239749	145.2	0.1342	0.0007	2.4	Moss, unidentifiable	-28.30	16,135	45	19,350	19,600	19,500
OS-164808	145.2	0.2169	0.0019	2.4	Moss, unidentifiable	-26.79	12,300	70	14,050	14,850	14,300
UCIAMS-239748	181.0-182.5	0.1949	0.0006	6.8	*Drepanocladus*, *Paludella squarrosa*, *Potomegeton*, unidentifiable	-19.40	13,135	30	15,650	15,900	[a]15,750
UCIAMS-239746	185.5-188.5	0.1875	0.0006	2.1	Moss, *Potomegeton*, unidentifiable	-14.60	13,450	25	16,050	16,300	[a]16,200
UCIAMS-239745	239.0-241.5	0.1910	0.0009	2.5	Unidentifiable	NA	13,300	40	15,800	16,150	[a]16,000
OS-162874	255.0	0.2029	0.0020	2.5	Moss, unidentifiable	-26.60	12,800	80	15,050	15,550	15,300
Vincent-3 (20VIN3)											
UCIAMS-239753	34.5-35.5	0.1988	0.0006	25.8	*Chara*, unidentifiable	-15.30	12,980	25	15,350	15,650	[a]15,550
OS-162873	146.5-152.0	0.2100	0.0020	2.1	Unidentifiable	-26.56	12,550	75	14,350	15,150	14,850
Vincent-4 (20VIN4)											
UCIAMS-239752	17.0-18.0	0.2126	0.0007	5.1	Beetle wing, *Cladocera*, *Chara*, unidentifiable	-24.90	12,435	30	14,300	14,900	14,550
UCIAMS-239751	87.0-88.0	0.2127	0.0010	39.2	Unidentifiable	NA	12,435	40	14,300	14,900	14,550
UCIAMS-239750	97.5-98.8	0.2150	0.0011	6.3	Unidentifiable	NA	12,350	45	14,150	14,850	14,400
OS-162875	174.0-175.0	0.2120	0.0019	2.0	Twig	-27.97	12,450	75	14,250	15,000	14,600
Songster (21SONG1)											
OS-160884	39.3	0.2107	0.0015	6.4	Bark (likely *Picea*)	NA	12,500	55	14,350	15,050	14,700
Allenberg (15ABB7)											
OS-123347	971.0	0.8877	0.0019	NA	Not identified	-25.96	955	20	795	920	850

continued

https://doi.org/10.5194/egusphere-2023-2655
Preprint. Discussion started: 5 February 2024

OS-123426	1178.0	0.4580	0.0018	NA	Not identified	-27.09	6,270	30	7,030	7,270	7,210		
OS-123427	1295.0	0.2607	0.0020	NA	Not identified	-26.82	10,800	60	12,700	12,850	12,750		
OS-123348	1456.0	0.2227	0.0012	NA	Not identified	-24.62	12,050	40	13,800	14,050	13,900		
Little Protection (21LPB1)													
OS-163424	53.7	0.5464	0.0014	4.6	Wood	-24.58	4,860	20	5,490	5,650	5,590		
OS-163425	141.0	0.4549	0.0017	15.6	Wood	-28.34	6,330	30	7,170	7,320	7,250		
OS-163426	198.5	0.4376	0.0013	39.7	Wood	-27.97	6,640	25	7,430	7,570	7,530		
OS-163427	320.5	0.3295	0.0012	5.4	*Potomegeton*	-17.55	8,920	30	9,900	10,200	[a]10,050		
OS-163428	423.0	0.3034	0.0015	5.8	Seed pod	-27.98	9,580	40	10,750	11,150	10,950		
OS-163517	472.2	0.2512	0.0016	5.5	*Picea* cone	-25.65	11,100	50	12,850	13,100	13,000		
OS-163500	481.0	0.2346	0.0017	32.9	Wood	-26.95	11,650	60	13,350	13,600	13,500		
OS-163501	493.0	0.2277	0.0015	3.0	Wood	-27.27	11,900	55	13,600	14,000	13,750		
OS-163429	511.0	0.1749	0.0023	11.0	Fish bone	-26.48	14,000	110	16,650	17,350	[a]17,000		
Dragonfly (13DFK1)													
OS-106743	25.2	0.6025	0.0031	NA	Twig	-22.80	4,070	40	4,420	4,800	4,560		
OS-106745	194.9	0.3381	0.0016	NA	Moss stems	-26.60	8,710	40	9,550	9,890	9,650		
OS-106746	362.4	0.3157	0.0017	NA	Moss stems	-25.00	9,260	45	10,300	10,550	10,450		
OS-133658	431.5	0.2729	0.0015	NA	Leaf	-25.70	10,450	45	12,100	12,600	12,350		
OS-106747	453.5	0.2704	0.0017	NA	Twig	-25.90	10,500	50	12,100	12,700	12,550		
OS-133659	482.5	0.2447	0.0016	NA	Wood	-25.60	11,300	50	13,100	13,300	13,200		
OS-106863	524.6	0.2428	0.0011	NA	Twig	-25.30	11,350	35	13,150	13,300	13,250		
OS-133660	541.6	0.2220	0.0015	NA	Twig	-25.70	12,100	55	13,800	14,100	13,950		
OS-107085	567.6	0.2048	0.0014	NA	Grass	-35.40	12,750	55	15,000	15,400	15,200		

[a] Samples not used in the discussion due to possible hardwater effect
NA: Not Available.
NA $\delta^{13}C$: Sample was either too small or the measurement was not requested.
NA Mass: Not recorded

https://doi.org/10.5194/egusphere-2023-2655
Preprint. Discussion started: 5 February 2024

4.3 Optically stimulated luminescence dating

Our small-aliquot D_e results from both 21SICK-01 and -02 show evidence of partial bleaching, as expected in a glaciofluvial environment (Table 3; AFig. 1 & 2; Rittenour et al., 2015). D_e results from the two samples are considerably scattered, positively skewed, and have overdispersion values between ~30 and ~60%, all indicative of incomplete bleaching and justify the use of the MAM (e.g., Olley et al. (1999). Our two OSL MAM ages are 19.8 ± 2.6 and 20.6 ± 2.9 ka. The two samples are from within 10 cm of each other and yield statistically indistinguishable ages.

Table 3. Optically Stimulated Luminescence Age Information

Sample num.	USU num.	Depth (m)	Num. of Analyses[1]	Dose Rate (Gy/kyr)	Equivalent Dose[2] ± 2σ (Gy)	OSL Age ± 1σ (ka)
21-SICK-1	USU-3622	2.05	21 (42)	2.70 ± 0.11	53.55 ± 11.51	**19.82 ± 2.60**
21-SICK-2	USU-3623	2.15	23 (37)	2.23 ± 0.09	46.09 ± 10.07	**20.63 ± 2.91**

[1] Age analysis using the single-aliquot regenerative-dose procedure of Murray and Wintle (2000) on 0.4-1-mm small-aliquots (SA) of quartz sand (150-250 µm). Number of aliquots used in age calculation and number of aliquots in parentheses.
[2] Equivalent dose (D_E) calculated using the Minimum Age Model (MAM) of Galbraith and Roberts (2012).

5 Discussion

5.1 Stratigraphy

We interpret Unit 1 as the primary till that comprises the Kent Moraine. At the Vincent-1 site we cored from 4.1 to 6.6 m below the wetland surface (2.5 m), but only recovered 1.2 m due to compaction with the GeoProbe system. We assume we reached below the post-glacial infill and into the primary glacial deposit since this unit spans 2.5 m and we found no changes in stratigraphy (Fig. 5).

Given the hummocky nature of the moraines (Fig. 3) and the complex stratigraphy within Unit 2 (Fig. 5), we interpret this unit to record the transition from an ice-cored moraine to the modern kettled topography for both moraines. The most striking feature of the sediment cores are the numerous transitions between fine- and coarse-grained deposition. We interpret Unit 2 silt settled out of suspension in lacustrine conditions, indicating that all seven basins likely held small kettle lakes of shifting dimension during this period. We propose that the alternating clay and diamicton sediments captured in 20VIN4 are slumps of primary till into the kettle lake with otherwise clay-rich sedimentation; these slumps probably occurred as buried glacial ice melted and destabilized the basin's slopes. The stratigraphy from 21LPB1 is likely the result of the changing depositional environments on the moraine as the kettle formed. Higher energy deposits of sand and gravel at the base of the unit were likely deposited atop the ice-cored moraine in fluvial or shallow water settings before being redeposited, in stratigraphic position, by the melting of buried ice beneath them. These sediments then floored the new kettle lake and deposition of lacustrine silt began.

https://doi.org/10.5194/egusphere-2023-2655
Preprint. Discussion started: 5 February 2024

The transition in sediment type between Units 2 and 3 likely reflects a shift to a more productive lake and landscape, in concert with increased stabilization of the surrounding moraine. Some layers of minerogenic sediment in the bottom of Unit 3 in 20VIN1 & 20VIN3 show that the landscape continued to receive sediment from primary glacial deposits after the transition to more organic-rich deposition. We infer that the inclusions of gray clay and brown silty macrofossils in 20VIN1 are rip-up clasts by their clast-like appearance and stark contrast to the surrounding sediment (Fig 5; Panel C). They were potentially frozen during the time of deposition. This further suggests the presence of reworked material near the Unit 2/3 transition. The subsequent transition from lacustrine organic-rich silt to peat (Lower and Upper Unit 3, respectively) records the shift from lake to bog/wetland due to the filling of the basin, shallowing of the lake, and encroachment of the shoreline.

5.2 Chronology

The OSL ages support our estimated age of 25 – 20 ka for the Kent Moraine from prior literature and affirms our confidence in the age assignments using correlations of dated features elsewhere. The OSL samples are from 2 m below the surface of the ~70 m thick kame delta. The sample location within the topset beds of a short-lived ice-contact delta suggests that our OSL samples constrain the time just before the ice sheet retreated and ceased building the delta 19.8 ± 2.6 – 20.6 ± 2.9 ka.

The basal ages, taken at face value, indicate the deposition of the Kent Moraine occurred shortly before ~15 ka; this does not agree with our OSL age or the regional correlations. Furthermore, a Kent Moraine age of ~15 ka contradicts the ~17 ka age for the Lake Escarpment Moraine, which lies up ice flow from the Kent Moraine. The above information, combined with our evidence for an unstable landscape depicted from our sediment core stratigraphy and numerous age reversals, suggests that our radiocarbon ages from Unit 2 consist of organic material that was reworked into these kettles during kettle formation.

We have identified spores and seeds of aquatic plants *Chara* and *Potamogeton* (O. Bennike, personal communication) among the macrofossils from samples 16,050-16,300 and 15,650-15,900 cal yr BP from 20VIN1 and sample 15,350-16,650 cal yr BP from 20VIN3. These samples also have enriched $\delta^{13}C$ values, suggesting that these samples contained aquatic material (Deuser and Degens, 1967; Oana and Deevey, 1960; Wang and Wooller, 2006). Our sites lie within calcareous tills that overlie sedimentary bedrock (LaFleur, 1979; MacClintock and Apfel, 1944), which can add aged carbon to the lake water. Aquatic plants derive their carbon from lake water, so radiocarbon ages from aquatic plants could produce radiocarbon ages that overestimate the age of the sample (the 'hardwater effect'; Deevey et al., 1954; Keeley and Sandquist, 1992).

We move forward using samples assumed to be terrestrial from visual identification and supported by $\delta^{13}C$ values. Four ages from 20VIN1 Unit 2 remain: 19,350-19,600, 15,050-15,550, 14,300-15,050, and 14,050-14,850 cal yr BP. We limit the 20VIN3 chronology to one trustworthy age of 14,350-15,150 cal yr BP. We derived the age of 16,650-17,350 cal yr BP in 21LPB1 from a fish bone; a fish could be susceptible to the same hardwater effect as aquatic vegetation, and thus we do not use it in our evaluation. Instead, we use the next lowest age of 13,600-14,000 cal yr BP as the basal age, along with 15,000-15,400 cal yr BP from 13DFK1.

https://doi.org/10.5194/egusphere-2023-2655
Preprint. Discussion started: 5 February 2024

These age estimates that are assumed to be more trustworthy still exhibit age reversals. These ages support our interpretation from the visual stratigraphy that reworked sediments contain organic matter that does not accurately date to the sediment's deposition. The macrofossil-rich rip-up clast in 20VIN1 holds evidence for two important interpretations: 1) the landscape was ice-free and at least sparsely vegetated as early as 19,350-19,600 cal yr BP (consistent with our OSL ages suggesting ice sheet retreat by 19.8 ± 2.6 – 20.6 ± 2.9 ka), and 2) the landscape stored this long-dead vegetation for thousands of years before it was redeposited.

Since we do not trust that radiocarbon ages from Unit 2 accurately date the time of sediment deposition, and the moraine ages are incompatible with regional correlations, we do not interpret our lowest, basal ages to record the timing of ice recession and abandonment of the moraines. Instead, we interpret these younger than expected ages to record kettle basin formation and moraine stabilization for both the Kent and Lake Escarpment moraines between 15,000-15,4000 and 13,600-14,000 cal yr BP. This interpretation also reconciles the similar basal ages between both moraines that are likely several thousand years different in age.

5.3 A model for kettle basin formation

We propose the following post-glacial history in western New York (Fig. 6). The deposition of the Kent Moraine occurred at least 19.8 ± 2.6 – 20.6 ± 2.9 ka and the landform remained ice-cored for the ensuing 5 – 6 kyr. The deposition of the Lake Escarpment Moraine took place around 17 ka and likewise remained ice-cored for the next 2 – 3 kyr. The hummocky nature of the moraines indicate that they were ice-cored, and we suggest that persistent buried glacial ice prohibited stabilization until well after deposition. Our interpretation is that after ~15 ka buried ice began to melt, and morainal topography – including kettle basins – began to evolve more rapidly (Fig. 6 & 7). During the earliest stages of kettle basin formation, there was increased mobilization of sediments from within the uneven ice-rich topography. These initial sediments contained both re-worked and contemporary organic matter from the catchment and were deposited in our study sites as Unit 2. According to this interpretation, our radiocarbon ages do not record the initial deposition of these moraines, but instead its stabilization ~15 to 14 ka.

Ice-cored moraines can remain ice-cored for thousands of years after deposition due to sediment cover that insulates and preserves the buried ice (Florin and Wright, 1969). If the region is cold enough to support permafrost it may extend the duration that the moraine remains ice-cored (Clayton et al., 2001; Henriksen et al., 2003; Schomacker, 2008). Given that the kettles appear to have formed within ~1 kyr of each other, and their formation coincided with the warm Bølling/Allerød period, this suggests the climate during Heinrich Stadial 1 may have been cold enough to help preserve the ice.

https://doi.org/10.5194/egusphere-2023-2655
Preprint. Discussion started: 5 February 2024

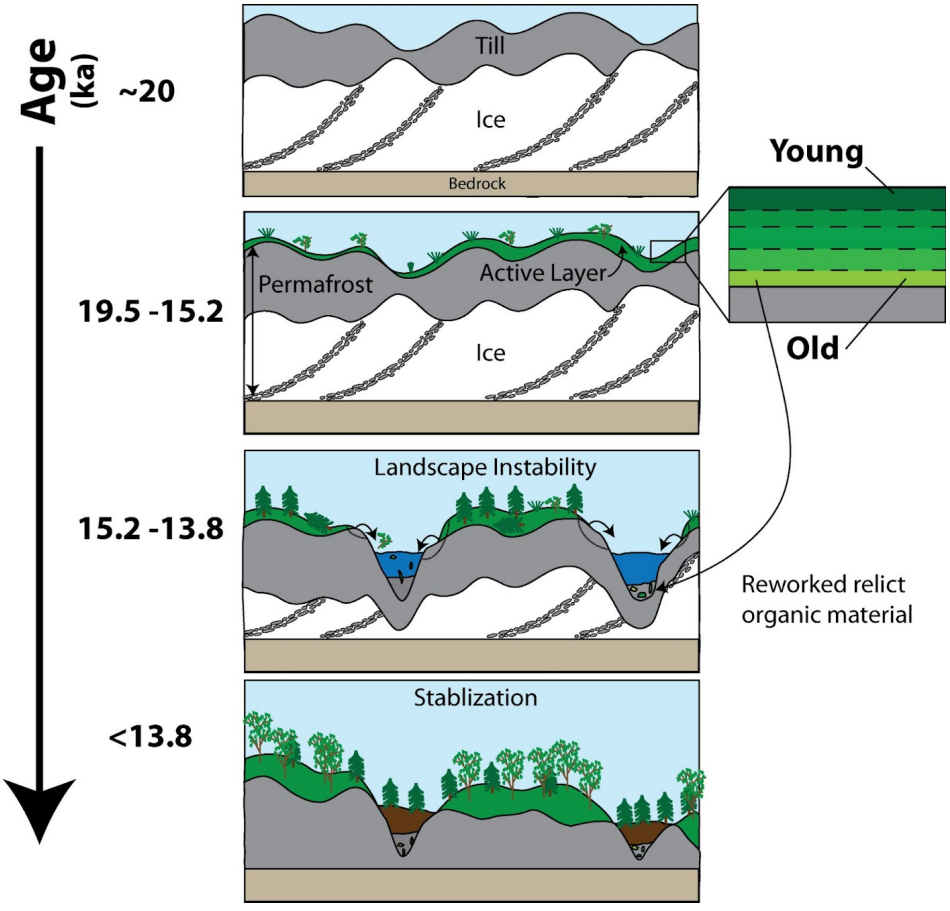

Figure 6. Conceptual model of kettle basin formation of the Kent Moraine in western New York building on Florin and Wright (1969). The same model applies to the Lake Escarpment moraine, except the timeline begins ~17 ka. First, the LIS deposited the ice-cored Kent Moraine. It remained ice-cored, perhaps influenced by permafrost, while tundra vegetation grew atop the moraine and stored carbon in the soil. Next, during climate amelioration in the Bølling-Allerød periods, the ice in the moraine melted. This led to the formation of basins that filled with both contemporaneous and reworked sediments. This is also likely the time when trees and other organic material could be slumped and formed deposits that placed primary tills adjacent to younger material. Finally, organic-rich sediment deposition dominates after ~13.8 ka.

5.4 Implications for the climate in western New York

The climate of western New York between 20 and 15 ka is poorly known, but records from Ontario, Ohio, and New England suggest the climate events of the North Atlantic influenced the northeastern U.S. These terrestrial climate reconstructions depict a cold Heinrich Stadial 1 (~18 to ~14.7 ka), a shift to warmer temperatures during the Bølling-Allerød, and a cool Younger Dryas (Gill et al., 2012; Gonzales and Grimm, 2009; Grigg et al., 2021; Shuman et al., 2002; Watson et al., 2018; Yu, 2007; Yu and Eicher, 1998). A stable Heinrich Stadial 1 and shift to

https://doi.org/10.5194/egusphere-2023-2655
Preprint. Discussion started: 5 February 2024

warmer temperatures during the Bølling-Allerød is shown by Watson et al. (2018), who used biomarkers (branched-GDGTs) to report that mean annual temperature in central Ohio varied between –2.0 and -0.5 °C from 17.0 to 14.5 ka before warming 5°C between 14.5 and 13.0 ka.

The rate of LIS retreat offers additional insight into the climate in the northeast US. Barth et al. (2019) used cosmogenic nuclide dating of glacially-transported boulders to estimate LIS thinning in the Adirondack Mountains and showed increased thinning between 15.4 ± 1.0 and 13.9 ± 0.9 ka, generally coincident with the Bølling. The New England Varve Chronology shows a relatively steady net retreat rate of the LIS through the Hudson Valley between 18 and 14.7 ka; during the Bølling the net retreat rate tripled, implying that New England experienced elevated warmth at that time (Ridge et al., 2012).

Ice-wedge casts can be used to identify areas that experienced past permafrost and constrain past temperature because their formation requires mean annual temperatures between -6 to -8°C (French, 2007; French and Miller, 2014). Ice-wedge casts are preserved in southern Ontario that were deposited 18-15 ka based on regional correlations (Dalton et al., 2020; Gao, 2005; Morgan et al., 1982). This suggests that the mean annual air temperature was low enough near our study site during Heinrich Stadial 1 to support permafrost. While this temperature depression is larger than reported by Watson et al. (2018), it's likely there was a strong temperature gradient between Ohio and western New York during deglaciation, with the latter remaining within 100 km of the ice margin until 14 ka (Dalton et al., 2020). This proximity to the ice sheet from the LGM to 14 ka may have been a driver of the cold climate that persisted in western New York. There are no reports of relict permafrost features within the LGM limit in western New York, but their presence south of the LGM extent suggest the likelihood of permafrost within the limit as well (French and Millar, 2014).

Finally, there are seven local pollen records from Miller (1973), Calkin and McAndrews (1980), and Doody (2018) that describe the initial deglacial vegetation in western New York. Only the Allenberg Bog (Miller, 1973) and Dragonfly Kettle (Doody, 2018) pollen records captured a ‘tundra’ zone at the base, although the presence of both arctic and temperate vegetation complicates their interpretation. Given our results, we believe this pollen tundra zone captured both the tundra vegetation that was growing on the moraine prior to basin formation and the more temperate vegetation as spruce and pine moved in during the Bølling. Unfortunately, the pollen records may be unreliable before 14 ka due to the same reworking problems as our radiocarbon dating, but this remains site specific. The tundra zone is overlain by an interval with high spruce and pine pollen; this is the lowest unit found in the other five records (Miller, 1973; Calkin and McAndrews, 1980). This is likely reflecting the new forest biome associated with warmer temperatures.

Altogether, there is evidence that the lag time between ice sheet retreat and kettle basin stabilization may be attributable to sustained permafrost in western New York due to cold North Atlantic conditions during Heinrich Stadial 1 (Fig. 7). The warming at the Bølling onset at ~14.7 ka may have increased regional temperatures, causing the melting of buried ice, initiating a phase of rapid landscape evolution and the formation of kettle basins, and eventually stabilizing the morainal topography. Numerous studies discuss the role of permafrost in the lag time between moraine ages and basal macrofossils along the south-central LIS margin, including Indiana and Illinois (Curry et al., 2018; Fisher et al., 2020), Michigan (Yansa et al., 2020), and Wisconsin (Clayton et al., 2008).

https://doi.org/10.5194/egusphere-2023-2655
Preprint. Discussion started: 5 February 2024

Our findings support the observations and conclusions from numerous studies that radiocarbon dates can be extreme minimum age constraints on deglaciation (Curry et al., 2018; Fisher et al., 2020; Florin and Wright, 1969; Halsted et al., 2023; Yansa et al., 2020). In New England, minimum-limiting radiocarbon ages may be the reason for the discrepancy between the timing of moraine deposition as recorded by ^{10}Be exposure dating (e.g., Balco et al., 2002; Corbett et al., 2017) and radiocarbon ages of basal macrofossils in lakes and bogs (e.g., Peteet et al., 2012). The younger than expected radiocarbon ages from the Valley Heads Moraine from Kozlowski et al. (2018) may be afflicted by similar processes. Permafrost during Heinrich Stadial 1 may have minimized landscape evolution in New England and central New York as well and could help explain the offset.

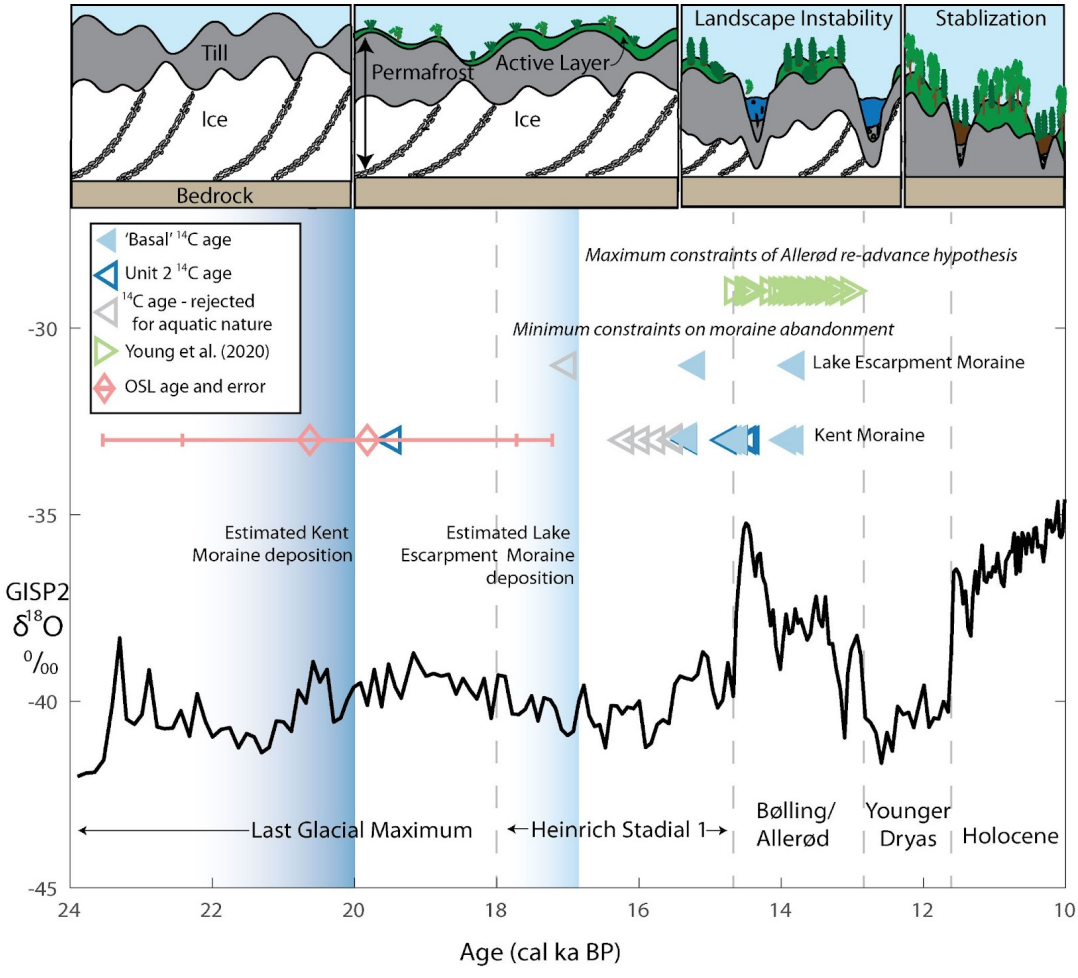

Figure 7. Comparison of radiocarbon ages from the Kent and Lake Escarpment moraine and Young et al. (2020) in the context of North Atlantic deglacial climate changes. Black line is the GISP2 $\delta^{18}O$ record (Grootes and Stuiver, 1999). Dark blue and light blue fading is the estimated deposition of the Kent Moraine and Lake Escarpment Moraine, respectively. Dark blue and light blue triangles are the lowest reliable radiocarbon ages from the Kent and Lake Escarpment Moraine sediment cores, respectively. Gray triangles are radiocarbon ages that we suspect have hardwater contamination. Pink diamonds are OSL ages and 2σ errors from the kame delta outboard the Kent Moraine. Green triangles are ages from

https://doi.org/10.5194/egusphere-2023-2655
Preprint. Discussion started: 5 February 2024

Young et al. (2020) interpreted by them to be maximum-limiting constraints on the 13 ka re-advance. Errors for all radiocarbon dates are not plotted because their width is smaller than the symbols.

5.5 Allerød re-advance hypothesis

The stratigraphically lowest radiocarbon ages from Unit 3 in the Lake Escarpment Moraine kettle basins, which are 15,000-15,400 and 13,600-14,000 cal yr BP, pre-date the ~13.1 ka re-advance suggested by Young et al. (2020) (Fig. 5 & 7). Chronologically constrained organic-rich sedimentation, with no stratigraphic evidence of interruption, ensued from at least 13,600-14,000 cal yr BP and well into the Holocene. Furthermore, there is no evidence of over-compaction in our bulk density measurements in 21LPB1 during this interval of time (Fig. 5). Thus, we do not find evidence that a ~13.1 ka LIS advance created or overran the Lake Escarpment Moraine as hypothesized by Young et al. (2020). Rather, we suggest that the landscape was unstable during its transition from a permafrost-dominated landscape to one with evolving and then stabilizing morainal topography. This landscape instability with reworking of glacial sediments may have led to the stratigraphy interpreted by Young et al. (2020) as primary tills in contact with trees dating to 13 ka (Fig. 7). Both the Dragonfly and Little Protection sites have intervals with increased wood deposition between 14 and 13 ka and future work could investigate the source of these woody intervals to further investigate the results from Young et al. (2020).

6 Conclusion

We present 41 new macrofossil-based radiocarbon ages from kettle basin infills in western New York. We find that the lowest reliable radiocarbon ages between 15,000-15,400 and 13,600-14,000 cal yr BP are 2 – 6 kyr younger than our OSL age constraints on moraine deposition of 19.8 ± 2.6 – 20.6 ± 2.9 ka. We interpret this offset to be due to a cold climate in western New York during Heinrich Stadial 1 supporting persistent buried ice which inhibited kettle basin formation until regional warming that took place during the Bølling. Our results do not support a re-advance of the LIS over the Lake Escarpment Moraine ~13 ka (c.f. Young et al., 2020). The lag time between ice sheet retreat and moraine stabilization in western New York may present an alternate explanation for inconsistencies between basal ages in sediment cores and other dating methods in central New York (Kozlowski et al., 2018) and eastern New York (Peteet et al., 2012).

Future work could target features that are stable during ice retreat even where permafrost is present, such as outcrops of pro-glacial and ice-walled lake plane deposits (e.g., Curry et al., 2018), or perhaps moraines that are not hummocky in nature. This limitation may not be as necessary in environments where climate more quickly ameliorated, such as appears to have been the case in southern Ohio (Glover et al., 2011). Additionally, it may be important to consider the coring equipment. The GeoProbe coring device enabled us to collect stiff mineral-rich sediments lower than otherwise possible with the Livingstone and Russian Peat coring devices. This meant that our coring did not stop at first contact with stiff minerogenic sediment that could mistakenly be interpreted as primary glacial in origin.

https://doi.org/10.5194/egusphere-2023-2655
Preprint. Discussion started: 5 February 2024

476 **Appendix A.**

Table A1: Dose Rate Information

USU num.	Lat/Long	In-situ H_2O (%)	D_R Subsample[1]	K (%)[2]	Rb (ppm)[2]	Th (ppm)[2]	U (ppm)[2]	Cosmic (Gy/kyr)
USU-3622	42.11394/ -78.94899	7.5	F: 70% M: 20% C: 10%	1.64±0.04 1.12±0.03 1.29±0.03	77.6±3.1 58.7±2.3 76.1±3.0	7.8±0.7 8.6±0.8 11.1±1.0	2.6±0.2 2.2±0.2 2.1±0.1	0.18±0.02
USU-3623	42.11394/ -78.94899	20.0	F: 85% M: 15%	1.52±0.04 1.35±0.03	74.4±3.0 72.7±2.9	8.3±0.7 8.4±0.8	2.0±0.1 2.4±0.2	0.18±0.02

[1] Dose rate (D_R) subsamples based on grain size: fine-F (<1.7 mm), medium-M (1.7-16 mm), coarse-C (>16 mm), and weighted proportions (%) of subsamples used with chemistry in gamma dose rate calculation. Beta dose rate uses chemistry from fine fraction (<1.7 mm) only.

[2] Radioelemental concentrations determined using ICP-MS and ICP-AES techniques; dose rate is derived from concentrations by conversion factors from Guérin et al. (2011).

477

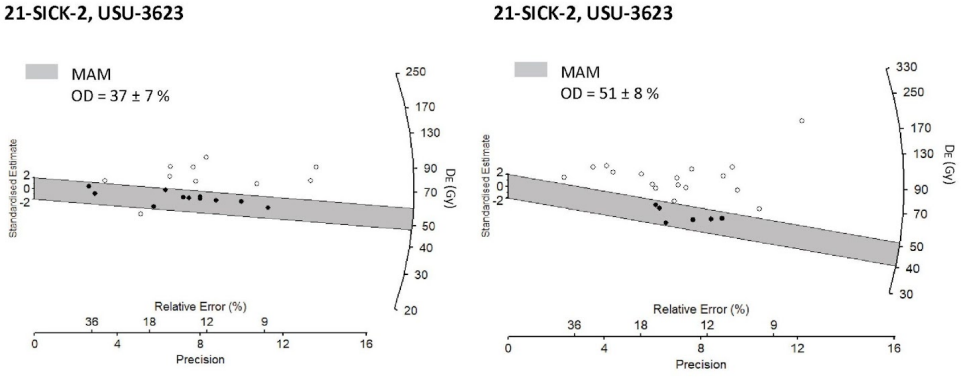

478

479 **Figure A1. Equivalent dose (D_E) distributions for the luminescence samples collected from the kame delta associated with**
480 **an ice-margin position near the Kent moraine. MAM = minimum age model of Galbraith and Roberts (2012) fit to the D_E**
481 **data (gray shaded region). OD = overdispersion, a metric of D_E scatter beyond instrumental error, where OD > 30% is**
482 **interpreted to be due to partial bleaching due to incomplete solar resetting of the luminescence signals in the quartz**
483 **grains.**

https://doi.org/10.5194/egusphere-2023-2655
Preprint. Discussion started: 5 February 2024

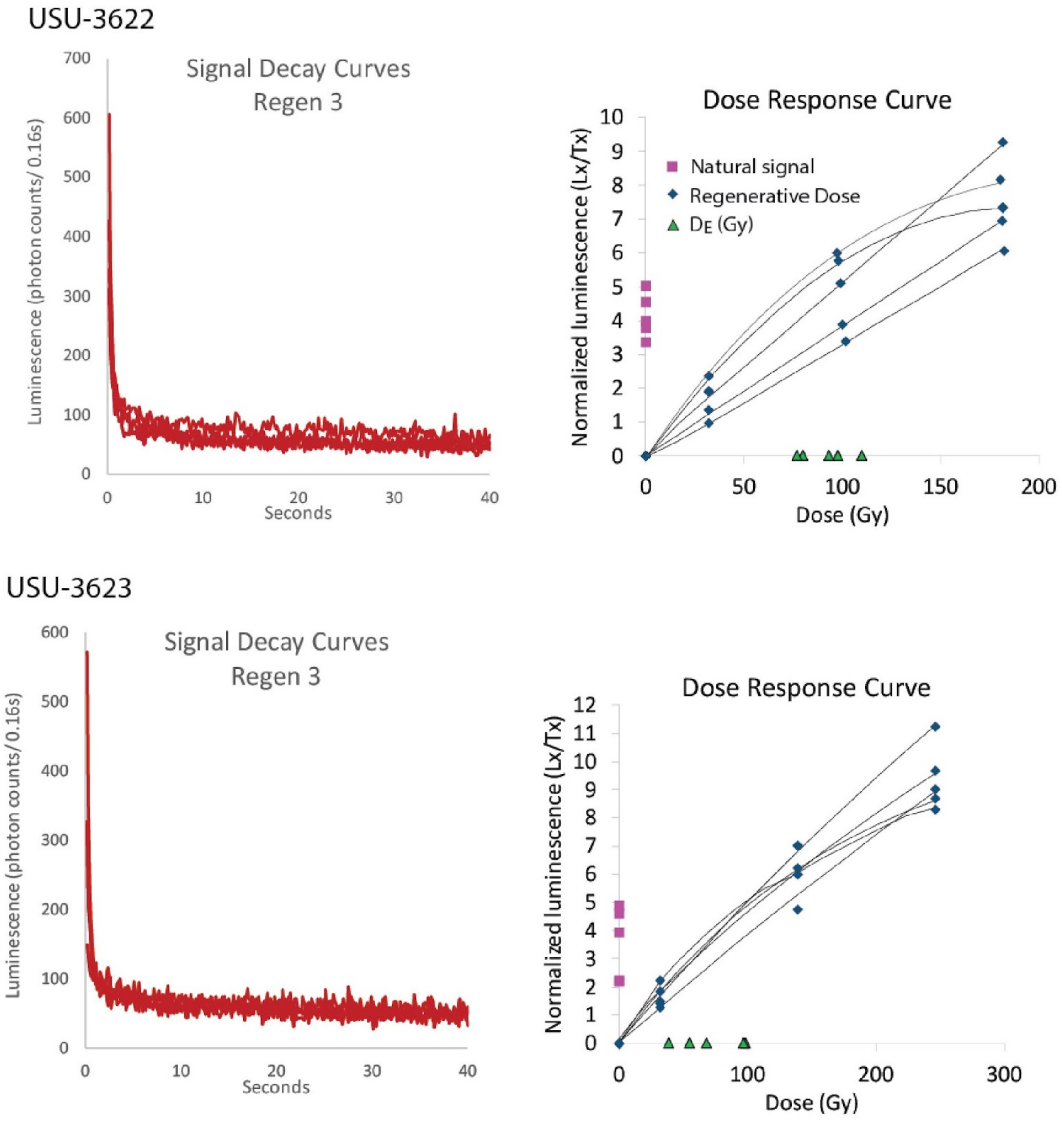

Figure A2. Example luminescence signal decay (left) and dose-response curves from 5 aliquots from each of the luminescence samples.

Data availability: Table 2 provides the data to calculate the radiocarbon ages from this study. Table 3 and Table A1 provide the data to calculate OSL ages from this study.

Author contributions: JPB and KKP conceptualized the study. ALK and KKP provided funding for fieldwork and lab analyses. KKP, JPB, CKW, BMC, and EPY collected sediment cores. KKP, BMC, EPY and JPB conducted

https://doi.org/10.5194/egusphere-2023-2655
Preprint. Discussion started: 5 February 2024

downcore analyses and radiocarbon sampling. CKW collected OSL samples and TMR conducted lab analyses and calculated the ages. KKP compiled and recalculated the radiocarbon ages. KKP, JPB, ALK, CKW, and BMC interpreted the results. KKP wrote the first draft of the manuscript and all authors contributed to editing. KKP and TMR developed the figures and tables.

Competing interests. The authors declare that they have no conflict of interest.

Acknowledgements: We thank the Vincent, Songster, Gebhard, and Bohall families for the access to their property, as well as their enthusiasm and friendship. We thank Joseph Tulenko, Brandon Graham, Elizabeth Thomas, Kurt Lindberg, Owen Cowling, Fiona Ellsworth, Joshua Charlton, Liza Wilson, Jason Parsons, Will Phillips, and George Thomas for their help in the field (it takes a village!). We thank the National Ocean Sciences Accelerator Mass Spectrometry and W. M. Keck Carbon Cycle Accelerator Mass Spectrometer laboratories for radiocarbon analyses. We thank the Luminescence Lab at Utah State University for OSL analyses.

Funding sources: This research was supported by the United State Geological Survey Great Lakes Geological Mapping Coalition grant #G20AC00418, the NSF/GSA Graduate Student Geoscience grant # 13056-21, which was funded by NSF Award # 1949901, and the Mark Diamond Research Fund of the Graduate Student Association of the State University of New York at Buffalo.

References

Balco, G., Stone, J. O. H., Porter, S. C., and Caffee, M. W.: Cosmogenic-nuclide ages for New England coastal moraines, Martha's Vineyard and Cape Cod, Massachusetts, USA, Quaternary Science Reviews, 21, 2127–2135, https://doi.org/10.1016/S0277-3791(02)00085-9, 2002.

Balco, G., Briner, J., Finkel, R. C., Rayburn, J. A., Ridge, C., and Schaefer, J. M.: Regional beryllium-10 production rate calibration for late-glacial northeastern North America, Quaternary Geochronology, 4, 93-107, https://doi.org/10.1016/j.quageo.2008.09.001, 2009.

Barth, A. M., Marcott, S. A., Licciardi, J. M., and Shakun, J. D.: Deglacial Thinning of the Laurentide Ice Sheet in the Adirondack Mountains, New York, USA, Revealed by 36Cl Exposure Dating, Paleoceanography and Paleoclimatology, 34, 946-953, https://doi.org/10.1029/2018PA003477, 2019.

Bird, B. and Kozlowski, A.: Late Quaternary Reconstruction of Lake Iroquois in the Ontario Basin of New York. New York State Museum Map & Chart 80, https://www.nysm.nysed.gov/sites/default/files/mc80_iroquois.pdf, 2016.

Briner, J. P., Cuzzone, J. K., Badgeley, J. A., Young, N. E., Steig, E. J., Morlighem, M., Schlegel, N. J., Hakim, G. J., Schaefer, J. M., Johnson, J. V., Lesnek, A. J., Thomas, E. K., Allan, E., Bennike, O., Cluett, A. A., Csatho, B., de

https://doi.org/10.5194/egusphere-2023-2655
Preprint. Discussion started: 5 February 2024

Vernal, A., Downs, J., Larour, E., and Nowicki, S.: Rate of mass loss from the Greenland Ice Sheet will exceed Holocene values this century, Nature, 586, 70-74, https://doi.org/10.1038/s41586-020-2742-6, 2020.

Broecker, W. S., Kennett, J. P., Flower, B. P., Teller, J. T., Trumbore, S., Bonani, G., and Wolfli, W.: Routing of meltwater from the Laurentide Ice Sheet during the Younger Dryas cold episode, Nature, 341, 318-321, https://doi.org/10.1038/341318a0, 1989.

Calkin, P. E. and Feenstra, B. H.: Evolution of the Erie-Basin Great Lakes, in: Quaternary Evolution of the Great Lakes, edited by: Karrow, P. F., and Calkin, P. E., Geological Society of Canada, https://doi.org/10.1016/0033-5894(87)90011-1, 1985.

Calkin, P. E. and McAndrews, J. H.: Geology and paleontology of two late Wisconsin sites in western New York State, Geological Society of America Bulletin, 91, 295-306, https://doi.org/10.1130/0016-7606(1980)91<295:GAPOTL>2.0.CO;2, 1980.

Campbell, M. C., Fisher, T. G., and Goble, R. J.: Terrestrial sensitivity to abrupt cooling recorded by aeolian activity in northwest Ohio, USA, Quaternary Research, 75, 411-416, https://doi.org/10.1016/j.yqres.2011.01.009, 2011.

Clayton, L. E., Attig, J. W., and Mickelson, D. M.: Effects of late Pleistocene permafrost on the landscape of Wisconsin, USA, Boreas, 30, 173-188, https://doi.org/10.1111/j.1502-3885.2001.tb01221.x, 2001.

Corbett, L. B., Bierman, P. R., Stone, B. D., Caffee, M. W., and Larsen, P. L.: Cosmogenic nuclide age estimate for Laurentide Ice Sheet recession from the terminal moraine, New Jersey, USA, and constraints on latest Pleistocene ice sheet history, Quaternary Research, 87, 482-498, https://doi.org/10.1017/qua.2017.11, 2017.

Coulombe, S., Fortier, D., Lacelle, D., Kanevskiy, M., and Shur, Y.: Origin, burial and preservation of late Pleistocene-age glacier ice in Arctic permafrost (Bylot Island, NU, Canada), The Cryosphere, 13, 97-111, https://doi.org/10.5194/tc-13-97-2019, 2019.

Cronin, T. M., Rayburn, J. A., Guilbault, J. P., Thunell, R., and Franzi, D. A.: Stable isotope evidence for glacial lake drainage through the St. Lawrence Estuary, eastern Canada, ~13.1-12.9 ka, Quaternary International, 260, 55-65, https://doi.org/10.1016/j.quaint.2011.08.041, 2012.

Curry, B. B., Lowell, T. V., Wang, H., and Anderson, A. C.: Revised time-distance diagram for the Lake Michigan Lobe, Michigan Subepisode, Wisconsin Episode, Illinois, USA, https://doi.org/10.1130/2018.2530(04), 2018.

Dalton, A. S., Margold, M., Stokes, C., Tarasov, L., Dyke, A., Adams, R., Allard, S., Arends, H., Atkinson, N., Attig, J., Barnett, P., Barnett, R., Batterson, M., Bernatchez, P., Borns, H., Breckenridge, A., Briner, J., Brouard, E., Campbell, J., and Wright, H.: An updated radiocarbon-based ice margin chronology for the last deglaciation of the

https://doi.org/10.5194/egusphere-2023-2655
Preprint. Discussion started: 5 February 2024

North American Ice Sheet Complex, Quaternary Science Reviews, 234, 106223, https://doi.org/10.1016/j.quascirev.2020.106223, 2020.

Deevey, E. S., Gross, M. S., Hutchinson, G. E., and Kraybill, H. L.: The Natural 14C Contents of Materials from Hard-Water Lakes, Proceedings of the National Academy of Sciences, 40, 285-288, https://doi.org/10.1073/pnas.40.5.285, 1954.

Deuser, W. G. and Degens, E. T.: Carbon Isotope Fractionation in the System CO2(gas)—CO2(aqueous)—HCO3−(aqueous), Nature, 215, 1033-1035, https://doi.org/10.1038/2151033a0, 1967.

Donnelly, J. P., Driscoll, N. W., Uchupi, E., Keigwin, L. D., Schwab, W. C., Thieler, E. R., and Swift, S. A.: Catastrophic meltwater discharge down the Hudson Valley: A potential trigger for the Intra-Allerød cold period, Geology, 33, https://doi.org/10.1130/G21043.1, 2005.

Doody, E.: A latest pleistocene palynologic record from western New York, Geology, University at Buffalo, 2018.

Dyke, A. S.: An outline of North American deglaciation with emphasis on central and northern Canada, in: Developments in Quaternary Sciences, edited by: Ehlers, J., and Gibbard, P. L., Elsevier, 373-424, https://doi.org/10.1016/S1571-0866(04)80209-4, 2004.

Elder, K. L., Roberts, M. L., Walther, T., and Xu, L.: Single step Production of graphite from organic Samples for Radiocarbon Measurements, Radiocarbon, 61, 1843-1854, https://doi.org/10.1017/RDC.2019.136, 2019.

Eschman, D. F. and Karrow, P. F.: Huron Basin Glacial Lakes: A Review, in: Quaternary Evolution of the Great Lakes, edited by: Karrow, P. F., and Calkin, P. E., Geological Society of Canada, https://doi.org/10.1016/0033-5894(87)90011-1, 1985.

Fairchild, H. L. R.: Glacial Waters in Central New York, University of the State of New York1909.

Fisher, T. G., Blockland, J. D., Anderson, A., Krantz, D. E., Stierman, D. J., and Goble, R.: Evidence of Sequence and Age of Ancestral Lake Erie Lake-Levels, Northwest Ohio, The Ohio Journal of Science 115, https://doi.org/10.18061/ojs.v115i2.4614, 2015.

Fisher, T. G., Dziekan, M. R., McDonald, J., Lepper, K., Loope, H., McCarthy, F. M. G., and Curry, B. B.: Minimum limiting deglacial ages for the out-of-phase Saginaw Lobe of the Laurentide Ice Sheet using optically stimulated luminescence (OSL) and radiocarbon methods, Quaternary Research, 97, 71-87, https://doi.org/10.1017/qua.2020.12, 2020.

Florin, M.-B. and Wright, H. E., Jr.: Diatom Evidence for the Persistence of Stagnant Glacial Ice in Minnesota, GSA Bulletin, 80, 695-704, https://doi.org/10.1130/0016-7606(1969)80[695:DEFTPO]2.0.CO;2, 1969.

https://doi.org/10.5194/egusphere-2023-2655
Preprint. Discussion started: 5 February 2024

French, H. M.: Surface Features of Permafrost, in: The Periglacial Environment, 116-152, https://doi.org/10.1002/9781118684931.ch6, 2007.

French, H. M. and Millar, S. W. S.: Permafrost at the time of the Last Glacial Maximum (LGM) in North America, Boreas, 43, 667-677, https://doi.org/10.1111/bor.12036, 2014.

Fritz, P., Morgan, A. V., Eicher, U., and McAndrews, J. H.: Stable isotope, fossil coleoptera and pollen stratigraphy in late quaternary sediments from Ontario and New York state, Palaeogeography, Palaeoclimatology, Palaeoecology, 58, 183-202, https://doi.org/10.1016/0031-0182(87)90059-9, 1987.

Fullerton, D. S.: Preliminary correlation of post-Erie interstadial events :(16,000-10,000 radiocarbon years before present), central and eastern Great Lakes region, and Hudson, Champlain, and St. Lawrence Lowlands, United States and Canada, https://doi.org/10.3133/pp1089, 1980.

Galbraith, R. F. and Roberts, R. G.: Statistical aspects of equivalent dose and error calculation and display in OSL dating: An overview and some recommendations, Quaternary Geochronology, 11, 1-27, https://doi.org/10.1016/j.quageo.2012.04.020, 2012.

Gao, C.: Ice-wedge casts in Late Wisconsinan glaciofluvial deposits, southern Ontario, Canada, Canadian Journal of Earth Sciences, 42, 2117-2126, https://doi.org/10.1139/e05-072, 2005.

Gao, C.: Relict Thermal-contraction-crack Polygons and Past Permafrost South of the Late Wisconsinan Glacial Limit in the Mid-Atlantic Coastal Plain, USA, Permafrost and Periglacial Processes, 25, 144-149, https://doi.org/10.1002/ppp.1803, 2014.

Gill, J. L., Williams, J. W., Jackson, S. T., Donnelly, J. P., and Schellinger, G. C.: Climatic and megaherbivory controls on late-glacial vegetation dynamics: a new, high-resolution, multi-proxy record from Silver Lake, Ohio, Quaternary Science Reviews, 34, 66-80, https://doi.org/10.1016/j.quascirev.2011.12.008, 2012.

Glover, K. C., Lowell, T. V., Wiles, G. C., Pair, D., Applegate, P., and Hajdas, I.: Deglaciation, basin formation and post-glacial climate change from a regional network of sediment core sites in Ohio and eastern Indiana, Quaternary Research, 76, 401-410, https://doi.org/10.1016/j.yqres.2011.06.004, 2011.

Gonzales, L. M. and Grimm, E. C.: Synchronization of late-glacial vegetation changes at Crystal Lake, Illinois, USA with the North Atlantic Event Stratigraphy, Quaternary Research, 72, 234-245, https://doi.org/10.1016/j.yqres.2009.05.001, 2009.

Grigg, L. D., Engle, K. J., Smith, A. J., Shuman, B. N., and Mandl, M. B.: A multi-proxy reconstruction of climate during the late-Pleistocene to early Holocene transition in the northeastern, USA, Quaternary Research, 102, 188-204, https://doi.org/10.1017/qua.2020.127, 2021.

https://doi.org/10.5194/egusphere-2023-2655
Preprint. Discussion started: 5 February 2024

615 Grootes, P. M. and Stuiver, M.: GISP2 Oxygen Isotope Data, PANGAEA [dataset],
616 https://doi.org/10.1594/PANGAEA.56094, 1999.

617 Halsted, C. T., Bierman, P. R., Shakun, J. D., Davis, P. T., Corbett, L. B., Drebber, J. S., and Ridge, J. C.: A critical
618 re-analysis of constraints on the timing and rate of Laurentide Ice Sheet recession in the northeastern United States,
619 Journal of Quaternary Science, https://doi.org/10.1002/jqs.3563, 2023.

620 Heath, S. L., Loope, H. M., Curry, B. B., and Lowell, T. V.: Pattern of southern Laurentide Ice Sheet margin position
621 changes during Heinrich Stadials 2 and 1, Quaternary Science Reviews, 201, 362-379,
622 https://doi.org/10.1016/j.quascirev.2018.10.019, 2018.

623 Heiri, O., Lotter, A. F., and Lemcke, G.: Loss on ignition as a method for estimating organic and carbonate content
624 in sediments: reproducibility and comparability of results, Journal of Paleolimnology, 25, 101-110,
625 https://doi.org/10.1023/A:1008119611481, 2001.

626 Henriksen, M., Mangerud, J., Matiouchkov, A., Paus, A., and Svendsen, J. I.: Lake stratigraphy implies an 80 000 yr
627 delayed melting of buried dead ice in northern Russia, Journal of Quaternary Science, 18, 663-679,
628 https://doi.org/10.1002/jqs.788, 2003.

629 Higley, M. C., Fisher, T. G., Jol, H. M., Lepper, K., and Martin-Hayden, J. M.: Stratigraphic and chronologic
630 analysis of the Warren Beach, northwest Ohio, USA, Canadian Journal of Earth Sciences, 51, 737-749,
631 https://doi.org/10.1139/cjes-2014-0047, 2014.

632 Keeley, J. E. and Sandquist, D. R.: Carbon: freshwater plants, Plant Cell & Environment, 15,
633 https://doi.org/10.1111/j.1365-3040.1992.tb01653.x, 1992.

634 Kozlowski, A. L., Bird, B. C., Lowell, T. V., Smith, C. A., Feranec, R. S., and Graham, B. L.: Minimum age of the
635 Mapleton, Tully, and Labrador Hollow moraines indicates correlation with the Port Huron Phase in central New
636 York State, in: Quaternary Glaciation of the Great Lakes Region: Process, Landforms, Sediments, and Chronology,
637 https://doi.org/10.1130/2018.2530(10), 2018.

638 LaFleur, R. G.: Glacial geology and stratigraphy of Western New York Nuclear Service Center and vicinity,
639 Cattaraugus and Erie Counties, New York, Report 79-989, https://doi.org/10.3133/ofr79989, 1979.

640 Last, W. and Smol, J.: Tracking environmental change using lake sediments. 2. Physical and geochemical methods,
641 https://doi.org/10.1007/0-306-47670-3, 2001.

642 Lewis, C. F. M. and Anderson, T. W.: A younger glacial Lake Iroquois in the Lake Ontario basin, Ontario and New
643 York: re-examination of pollen stratigraphy and radiocarbon dating, Canadian Journal of Earth Sciences, 57,
644 453-463, https://doi.org/10.1139/cjes-2019-0076, 2019.

https://doi.org/10.5194/egusphere-2023-2655
Preprint. Discussion started: 5 February 2024

Leydet, D. J., Carlson, A. E., Teller, J. T., Breckenridge, A., Barth, A. M., Ullman, D. J., Sinclair, G., Milne, G. A., Cuzzone, J. K., and Caffee, M. W.: Opening of glacial Lake Agassiz's eastern outlets by the start of the Younger Dryas cold period, Geology, 46, 155-158, https://doi.org/10.1130/G39501.1, 2018.

Löfverström, M., Caballero, R., Nilsson, J., and Kleman, J.: Evolution of the large-scale atmospheric circulation in response to changing ice sheets over the last glacial cycle, Climate of the Past, 10, 1453-1471, https://doi.org/10.5194/cp-10-1453-2014, 2014.

Lusch, D. P., Stanley, K. E., Schaetzl, R. J., Kendall, A. D., Van Dam, R. L., Nielsen, A., Blumer, B. E., Hobbs, T. C., Archer, J. K., Holmstadt, J. L. F., and May, C. L.: Characterization and Mapping of Patterned Ground in the Saginaw Lowlands, Michigan: Possible Evidence for Late-Wisconsin Permafrost, Annals of the Association of American Geographers, 99, 445-466, https://doi.org/10.1080/00045600902931629, 2009.

MacClintock, P. and Apfel, E. T.: Correlation of the drifts of the Salamanca re-entrant, New York, Bulletin of the Geological Society of America, 55, 1143-1164, https://doi.org/10.1130/GSAB-55-1143, 1944.

Miller, N. G.: Late-glacial and postglacial vegetation change in southwestern New York State, University of the State of New York, State Education Dept, Albany, https://www.biodiversitylibrary.org/bibliography/135533, 1973.

Morgan, A. V.: Distribution and probable age of relict permafrost features in south-western Ontario, 4th Canadian Permafrost Conference, Ottawa, Ontario, 91-100,

Muller, E. H. and Calkin, P. E.: Timing of Pleistocene glacial events in New York State, Canadian Journal of Earth Sciences, 30, 1829-1845, https://doi.org/10.1139/e93-161, 1993.

Muller, E. H. and Prest, V. K.: Glacial Lakes in the Ontario Basin, in: Quaternary Evolution of the Great Lakes edited by: Karrow, P. F., and Calkin, P., E.,, Geological Society of Canada, https://doi.org/10.1016/0033-5894(87)90011-1, 1985.

Murray, A. S. and Wintle, A. G.: Luminescence dating of quartz using an improved single-aliquot regenerative-dose protocol, Radiation Measurements, 32, 57-73, https://doi.org/10.1016/S1350-4487(99)00253-X, 2000.

Oana, S. and Deevey, E. S.: Carbon 13 in lake waters and its possible bearing on paleolimnology, American Journal of Science, 258-A, 253-272, 1960.

Olley, J. M., Caitcheon, G. G., and Roberts, R. G.: The origin of dose distributions in fluvial sediments, and the prospect of dating single grains from fluvial deposits using optically stimulated luminescence, Radiation Measurements, 30, 207-217, https://doi.org/10.1016/S1350-4487(99)00040-2, 1999.

Olsson, I.: Radiometric Methods, in: Handbook of Holocene paleoecology and paleohydrology, edited by: Berglund, B., John Wiley & Sons, Chichester, 273-312, https://doi.org/10.1002/gea.3340040208, 1986.

https://doi.org/10.5194/egusphere-2023-2655
Preprint. Discussion started: 5 February 2024

675 Osman, M. B., Tierney, J. E., Zhu, J., Tardif, R., Hakim, G. J., King, J., and Poulsen, C. J.: Globally resolved surface
676 temperatures since the Last Glacial Maximum, Nature, 599, 239-244, https://doi.org/10.1038/s41586-021-03984-4,
677 2021.

678 Pearson, A., McNichol, A. P., Schneider, R. J., Von Reden, K. F., and Zheng, Y.: Microscale AMS 14C Measurement
679 at NOSAMS, Radiocarbon, 40, 61-75, https://doi.org/10.1017/S0033822200017902, 1997.

680 Peteet, D. M., Beh, M., Orr, C., Kurdyla, D., Nichols, J., and Guilderson, T.: Delayed deglaciation or extreme Arctic
681 conditions 21-16 cal. kyr at southeastern Laurentide Ice Sheet margin?, Geophysical Research Letters, 39, n/a-n/a,
682 https://doi.org/10.1029/2012GL051884, 2012.

683 Porreca, C., Briner, J. P., and Kozlowski, A.: Laurentide ice sheet meltwater routing along the Iro-Mohawk River,
684 eastern New York, USA, Geomorphology, 303, 155-161, https://doi.org/10.1016/j.geomorph.2017.12.001, 2018.

685 Ramsey, K.: Geologic map of New Castle county, Delaware: Delaware Geological Survey Geologic Map Series, 13,
686 2005.

687 Ramsey, K.: Geologic map of Kent County, Delaware: Delaware Geological Survey Geologic Map Series, 2007.

688 Rayburn, J. A., Franzi, D. A., and Knuepfer, P. L. K.: Evidence from the Lake Champlain Valley for a later onset of
689 the Champlain Sea and implications for late glacial meltwater routing to the North Atlantic, Palaeogeography,
690 Palaeoclimatology, Palaeoecology, 246, 62-74, https://doi.org/10.1016/j.palaeo.2006.10.027, 2007.

691 Rayburn, J. A., K. Knuepfer, P. L., and Franzi, D. A.: A series of large, Late Wisconsinan meltwater floods through
692 the Champlain and Hudson Valleys, New York State, USA, Quaternary Science Reviews, 24, 2410-2419,
693 https://doi.org/10.1016/j.quascirev.2005.02.010, 2005.

694 Rayburn, J. A., Cronin, T. M., Franzi, D. A., Knuepfer, P. L. K., and Willard, D. A.: Timing and duration of North
695 American glacial lake discharges and the Younger Dryas climate reversal, Quaternary Research, 75, 541-551,
696 https://doi.org/10.1016/j.yqres.2011.02.004, 2011.

697 Reimer, P. J., Austin, W. E. N., Bard, E., Bayliss, A., Blackwell, P. G., Bronk Ramsey, C., Butzin, M., Cheng, H.,
698 Edwards, R. L., Friedrich, M., Grootes, P. M., Guilderson, T. P., Hajdas, I., Heaton, T. J., Hogg, A. G., Hughen, K.
699 A., Kromer, B., Manning, S. W., Muscheler, R., Palmer, J. G., Pearson, C., van der Plicht, J., Reimer, R. W.,
700 Richards, D. A., Scott, E. M., Southon, J. R., Turney, C. S. M., Wacker, L., Adolphi, F., Büntgen, U., Capano, M.,
701 Fahrni, S. M., Fogtmann-Schulz, A., Friedrich, R., Köhler, P., Kudsk, S., Miyake, F., Olsen, J., Reinig, F., Sakamoto,
702 M., Sookdeo, A., and Talamo, S.: The IntCal20 Northern Hemisphere Radiocarbon Age Calibration Curve (0–55 cal
703 kBP), Radiocarbon, 62, 725-757, https://doi.org/10.1017/RDC.2020.41, 2020.

https://doi.org/10.5194/egusphere-2023-2655
Preprint. Discussion started: 5 February 2024

Richard, P. J. H. and Occhietti, S.: 14C chronology for ice retreat and inception of Champlain Sea in the St. Lawrence Lowlands, Canada, Quaternary Research, 63, 353-358, https://doi.org/10.1016/j.yqres.2005.02.003, 2005.

Ridge, J. C.: The last deglaciation of the northeastern United States: a combined varve, paleomagnetic, and calibrated 14C chronology, in: Geoarchaeology of landscapes in the glaciated northeast, edited by: Hart, J. P., and Cremeens, D. L., New York State Museum Bulletin, 15-45, 2003.

Ridge, J. C., Balco, G., Bayless, R. L., Beck, C. C., Carter, L. B., Dean, J. L., Voytek, E. B., and Wei, J. H.: The new North American Varve Chronology: A precise record of southeastern Laurentide Ice Sheet deglaciation and climate, 18.2-12.5 kyr BP, and correlations with Greenland ice core records, American Journal of Science, 312, 685-722, https://doi.org/10.2475/07.2012.01, 2012.

Rittenour, T. M., Cotter, J. F. P., and Arends, H. E.: Application of single-grain OSL dating to ice-proximal deposits, glacial Lake Benson, west-central Minnesota, USA, Quaternary Geochronology, 30, 306-313, https://doi.org/10.1016/j.quageo.2015.02.025, 2015.

Schomacker, A.: What controls dead-ice melting under different climate conditions? A discussion, Earth-Science Reviews, 90, 103-113, https://doi.org/10.1016/j.earscirev.2008.08.003, 2008.

Shah Walter, S. R., Gagnon, A. R., Roberts, M. L., McNichol, A. P., Gaylord, M. C. L., and Klein, E.: Ultra-Small Graphitization Reactors for Ultra-Microscale 14C Analysis at the National Ocean Sciences Accelerator Mass Spectrometry (NOSAMS) Facility, Radiocarbon, 57, 109-122, https://doi.org/10.2458/azu_rc.57.18118, 2015.

Shuman, B., Webb Iii, T., Bartlein, P., and Williams, J. W.: The anatomy of a climatic oscillation: vegetation change in eastern North America during the Younger Dryas chronozone, Quaternary Science Reviews, 21, 1777-1791, https://doi.org/10.1016/S0277-3791(02)00030-6, 2002.

Stanford, S. D., Stone, B. D., Ridge, J. C., Witte, R. W., Pardi, R. R., and Reimer, G. E.: Chronology of Laurentide glaciation in New Jersey and the New York City area, United States, Quaternary Research, 1-26, https://doi.org/10.1017/qua.2020.71, 2020.

Stuiver, M. and Polach, H. A.: Discussion Reporting of 14C Data, Radiocarbon, 19, 355-363, https://doi.org/10.1017/S0033822200003672, 1977.

Stuiver, M. and Reimer, P. J.: Extended 14C Data Base and Revised CALIB 3.0 14C Age Calibration Program, Radiocarbon, 35, 215-230, https://doi.org/10.1017/S0033822200013904, 1993.

Teller, J. T.: Controls, history, outbursts, and impact of large late-Quaternary proglacial lakes in North America, in: The Quaternary Period in the United States, Developments in Quaternary Sciences, 45-61, https://doi.org/10.1016/S1571-0866(03)01003-0, 2003.

https://doi.org/10.5194/egusphere-2023-2655
Preprint. Discussion started: 5 February 2024

734 Terasmae, J.: Some problems of late Wisconsin history and geochronology in southeastern Ontario, Canadian
735 Journal of Earth Sciences, 17, 361-381, https://doi.org/10.1139/e80-035, 1980.

736 Tulenko, J. P., Lofverstrom, M., and Briner, J. P.: Ice sheet influence on atmospheric circulation explains the patterns
737 of Pleistocene alpine glacier records in North America, Earth and Planetary Science Letters, 534, 116115,
738 https://doi.org/10.1016/j.epsl.2020.116115, 2020.

739 US Geological Survey: FGDC Digital Cartographic Standard for Geologic Map Symbolization (PostScript
740 Implementation), http://pubs.usgs.gov/tm/2006/11A02/, 2006.

741 Vogel, J. S., Southon, J. R., Nelson, D. E., and Brown, T. A.: Performance of catalytically condensed carbon for use
742 in accelerator mass spectrometry, Nuclear Instruments and Methods in Physics Research Section B: Beam
743 Interactions with Materials and Atoms, 5, 289-293, https://doi.org/10.1016/0168-583X(84)90529-9, 1984.

744 Wang, Y. and Wooller, M. J.: The stable isotopic (C and N) composition of modern plants and lichens from northern
745 Iceland: with ecological and paleoenvironmental implications, Jökull, 56, 27-38, 10.33799/jokull2006.56.027, 2006.

746 Watson, B. I., Williams, J. W., Russell, J. M., Jackson, S. T., Shane, L., and Lowell, T. V.: Temperature variations in
747 the southern Great Lakes during the last deglaciation: Comparison between pollen and GDGT proxies, Quaternary
748 Science Reviews, 182, 78-92, https://doi.org/10.1016/j.quascirev.2017.12.011, 2018.

749 Wright, H. E. and Stefanova, I.: Plant trash in the basal sediments of glacial lakes, Acta Palaeobotanica, 44, 141-146,
750 2004.

751 Yansa, C. H., II, F. A. E., Schaetzl, R. J., Kettle, J. M., and Arbogast, A. F.: Interpreting basal sediments and plant
752 fossils in kettle lakes: insights from Silver Lake, Michigan, USA, Canadian Journal of Earth Sciences, 57, 292-305,
753 https://doi.org/10.1139/cjes-2018-0338, 2020.

754 Young, R. A., Gordon, L. M., Owen, L. A., Huot, S., and Zerfas, T. D.: Evidence for a late glacial advance near the
755 beginning of the Younger Dryas in western New York State: An event postdating the record for local Laurentide ice
756 sheet recession, Geosphere, https://doi.org/10.1130/GES02257.1, 2020.

757 Yu, Z.: Rapid response of forested vegetation to multiple climatic oscillations during the last deglaciation in the
758 northeastern United States, Quaternary Research, 67, 297-303, https://doi.org/10.1016/j.yqres.2006.08.006, 2007.

759 Yu, Z. and Eicher, U.: Abrupt Climate Oscillations During the Last Deglaciation in Central North America, Science,
760 282, 2235-2238, doi:10.1126/science.282.5397.2235, 1998.